

REVIEW

Dual doping: An emerging strategy to construct efficient metal catalysts for water electrolysis

Zhijie Chen¹  | Ning Han² | Wei Wei³ | Dewei Chu⁴ | Bing-Jie Ni¹

¹School of Civil and Environmental Engineering, The University of New South Wales, Sydney, New South Wales, Australia

²Department of Materials Engineering, KU Leuven, Leuven, Belgium

³Center for Technology in Water and Wastewater, School of Civil and Environmental Engineering, University of Technology Sydney, Ultimo, New South Wales, Australia

⁴School of Materials Science and Engineering, University of New South Wales, Sydney, New South Wales, Australia

Correspondence

Bing-Jie Ni.

Email: bingjieni@gmail.com

Funding information

Australian Research Council, Grant/Award Number: DP220101139

Abstract

Developing efficient electrocatalysts for water electrolysis is critical for sustainable hydrogen energy development. For enhancing the catalytic performance of metal catalysts, dual doping has attracted enormous interest for its high effectiveness and facile realization. Dual doping is effective for tuning the electronic properties, enhancing the electrical conductivity, populating active sites, and improving the stability of metal catalysts. In this review, recent developments in cation–cation, cation–anion, and anion–anion dual-doped catalysts for water splitting are comprehensively summarized and discussed. An emphasis is put on illustrating how dual doping regulates the external and internal properties and boosts the catalytic performance of catalysts. Additionally, perspectives are pointed out to guide future research on engineering high-performance heteroatom-doped electrocatalysts.

KEYWORDS

catalyst design, electrocatalysts, electronic structure, hydrogen evolution reaction, oxygen evolution reaction

1 | INTRODUCTION

Hydrogen energy is important for the decarbonization of global energy sectors owing to its features of zero-carbon footprint, high energy density, as well as high earth abundance.^{1–3} To meet the sharply growing demand for green hydrogen fuels, water electrolysis attracts growing interest. Water electrolysis consists of anodic oxygen evolution reaction (OER) and cathodic hydrogen

evolution reaction (HER), and the hydrogen production efficiency is largely determined by the applied electrocatalysts.^{4,5} Catalysts can be used to reduce reaction energy barriers and boost reaction kinetics.^{6,7} In this context, designing high-performance catalysts is vital for accelerating hydrogen energy development.

Redox-active metal materials have been extensively applied for water electrolysis for their high activity and good stability, especially Fe/Co/Ni/Ir/Ru/Pt-based

This is an open access article under the terms of the [Creative Commons Attribution](https://creativecommons.org/licenses/by/4.0/) License, which permits use, distribution and reproduction in any medium, provided the original work is properly cited.

© 2024 The Authors. *EcoEnergy* published by John Wiley & Sons Australia, Ltd on behalf of China Chemical Safety Association.

materials.^{8–13} The catalytic performance of metal catalysts is largely governed by their chemical compositions, electronic properties, and nanostructures.^{14,15} This feature provides great opportunities for researchers to develop high-performance catalysts by altering the physicochemical and electronic properties of metal materials. Besides improving the catalytic performance, lowering the catalyst cost is another key direction for sustainable water electrolysis. This can be achieved by reducing the utilization of noble metals and/or enhancing the intrinsic activity of active sites.^{16,17} Overall, developing cost-effective metal catalysts is important and diverse design strategies have been proposed recently, such as heteroatom doping,^{18–20} heterostructure construction,^{21,22} defect engineering,²³ nanostructure control,²⁴ and phase engineering.²⁵

Among all catalyst design strategies, heteroatom doping is an efficient and facile one to modulate the external and internal properties of electrocatalysts. Doping can help regulate electronic properties, improve electrical conductivity, populate the number of electroactive sites, and also enhance the stability of metal catalysts.^{26–28} For elevating the activity of heteroatom-doped catalysts, it is necessary to finely control their properties by optimizing the doping process. Compared with single elemental doping, dual doping that incorporates two different elements into metal catalysts is more effective in regulating the properties of metal catalysts.²⁹ Especially, dual doping can exploit the synergistic effect of the beneficial influences of the different heteroatoms and bring more space to regulate the properties of metal catalysts, thereby leading to finely controlled electronic structures, diverse catalytically active sites, etc.³⁰ For example, the co-presence of Ru and P dopants in NiMoO₄ leads to a lower work function than Ru-NiMoO₄, P-NiMoO₄, and NiMoO₄, evidencing facile electron migration in Ru/P co-doped NiMoO₄. In addition, the higher *d*-band center of Ru/P co-doped NiMoO₄ helps to promote the adsorption of reactants and accelerates the catalytic process.³¹ Hitherto, hundreds of cation–cation, cation–anion, and anion–anion dual-doped metal catalysts (e.g., metal oxides, metal chalcogenides, and metal pnictides) have been designed for OER, HER, and overall water electrolysis (OWS), and some of them exhibit promising performance for practical water electrolysis.^{32,33} Nevertheless, current developments in dual-doped electrocatalysts for water electrolysis have not been reviewed yet.

Herein, we comprehensively summarize recent accomplishments in the design of dual-doped metal electrocatalysts for water splitting. Water electrolysis mechanisms are not included here, which have been widely discussed in previous papers.^{34–36} The effects of dual doping on the properties of metal catalysts are examined. Afterward, current advances in developing

efficient dual-doped metal catalysts for water electrolysis are thoroughly discussed. Perspectives are further highlighted for guiding future studies on the design of efficient heteroatom-doped catalysts.

2 | EFFECTS OF DUAL DOPING ON METAL CATALYSTS' PROPERTIES

Dual doping emerges as a powerful approach to improve the catalytic performance of metal catalysts. Once the anion–anion, anion–cation, or cation–cation dopants are inserted into metal catalysts, the electronic interaction between dopants and atoms in the host materials can adjust the electronic properties of catalysts. This process can significantly increase the intrinsic activity and elevate the electrical conductivity of electrocatalysts. In addition, dopants can tune the nanostructure of metal catalysts, enlarging active surface area and providing more electroactive sites. Furthermore, dual doping has been suggested to enhance the stability of metal catalysts. In this section, the effects of dual doping on metal catalysts' properties are discussed.

2.1 | Regulating the electronic structure

Electronic structure is the most critical property that determines the intrinsic activity of metal catalysts. By incorporating heteroatoms into the lattice of catalysts, the electronic properties of catalysts will be regulated.³⁷ Compared with mono-doping, dual doping can finely tune the electronic properties of metal catalysts, realizing precise regulation of intrinsic activity. The electronic states, band structure, valence band, charge transfer capability, and adsorption capability of active sites can be changed upon dual doping.³⁸ For example, the dual Mn and Ni dopants in LaCoO₃ help to shift the valence band (*O 2p*) toward the Fermi level and improve the covalency of Co–O bonds, which benefits the OER process.³⁹ For water electrolysis, optimizing the binding energy of reaction intermediates (e.g., *OH, *H, and *OOH) is important for improving the catalytic reactions. This can be achieved by tuning the *d*-band center of catalysts, with the presence of dopants. Generally, the upshift of the *d*-band center can enhance the adsorption of reactants/intermediates, while the downshift of the *d*-band center leads to reduced adsorption strength of reactants/intermediates.⁴⁰ In a Co/Al co-doped Fe₂N/Fe₃N catalyst, the *d*-band center of Co/Al co-doped Fe₂N/Fe₃N (−1.011 eV) is lower than that of Al doped (−0.982 eV), Co doped (−0.928 eV), and undoped counterparts (−0.902 eV). Thus, more electrons are easily transferred into the antibonding states in Co/Al co-doped

Fe₂N/Fe₃N upon dual doping than other catalysts, resulting in lower H adsorption energy and adsorption energy of oxygen-containing intermediates toward achieving high HER and OER catalytic activities.⁴¹ Assisted by Density Functional Theory (DFT) calculations, one can tailor the *d*-band center of catalysts with suitable dual dopants.⁴² During the doping process, the dual dopants-induced lattice distortion also can introduce vacancies/defects.^{43,44} With a low-coordination number, these defective sites or the nearby active sites generally exhibit high intrinsic catalytic activity.⁴⁵

2.2 | Improving the electrical conductivity

In electrocatalytic processes, the electron transport efficiency of metal catalysts governs the catalytic performance largely. Doping can improve the electrical conductivity of metal catalysts by narrowing the band gap.^{46,47} Dual doping in semiconductor-type metal catalysts (e.g., metal oxides, hydroxides, and sulfides) offers high accessibility for improving their electrical conductivity. For instance, introducing dual rare earth metals (Ce, Sm, Yb, and Er) into Pr₂O₃ can enhance the electrical conductivity, as evidenced by the current-voltage measurements. Compared with the single Ce-doped Pr₂O₃, the introduction of a second rare earth dopant can reduce the electrical resistivity and lead to higher conductivity, and conductivity follows the order Pr₂CeO₃ < Pr₂CeYbO₃ < Pr₂CeErO₃ < Pr₂CeSmO₃.⁴⁸ For layered transition metal dichalcogenides (e.g., MoS₂ and MoTe₂), dual doping can enhance the conductivity by phase transformation. Compared with the 2H phase of MoTe₂, 1T, and 1T' phases have much better electrical conductivity.⁴⁹ Gao et al. found that Co/Ni co-doping could efficiently realize the MoTe₂ 2H-to-1T' transformation and lead to enhanced electrical conductivity.⁵⁰ The synergistic effect of Co and Ni dopants significantly decreased the energy barrier in the phase transition procedure by tuning the charge of host Mo atoms. Besides cation-involved dual doping processes, anion-anion dual doping (e.g., F/P co-doped NiSe₂⁵¹) can also enhance the conductivity of catalysts. Accordingly, dual doping can significantly augment the electrical conductivity of metal catalysts, therefore enhancing the charge-transfer process in electrocatalysis.

2.3 | Populating active sites

Aside from the intrinsic activity of per active site, the population of active sites is another essential issue that

governs the catalytic activity of electrocatalysts. Dual doping can populate the active sites by introducing active species and regulating the nanostructure of catalysts.⁵² When incorporating active elements (e.g., Fe, Co, Ni, S, and P) into metal catalysts, these dopants will act as electroactive sites for water electrolysis and thus increase the number of active sites. For instance, in the Mn/S co-doped Co₃O₄, the Mn dopant shifts the electronic structure of the Co site, and the S dopant can provide active S sites for the proton adsorption step.⁵³ Dual doping also can increase the active sites by shaping the morphology of electrocatalysts. Generally, open structures benefit the exposure of active sites and mass/charge transport. In the S/Fe co-doped NiMoO₄ catalyst, Fe²⁺ and S²⁻ ions in the precursor contribute to the formation of one-dimensional (1D) NiMoO₄ microrod arrays. Compared with the single Fe-doped sample with a messy structure, the dual-doped NiMoO₄ microrod arrays show lower charge transfer resistance (*R*_{ct}) and higher electroactive active surface area.⁵⁴ Similar dual doping-induced nanostructure regulation has been suggested by Mo/P co-doped NiCoO_x,⁵⁵ Mo/S co-doped NiSe₂,⁵⁶ Mo/O co-doped CoP,⁵⁷ Mo/N co-doped CoP,⁵⁸ etc.

2.4 | Enhancing the stability

Practical water electrolyzers need stable electrocatalysts that can work for a long time under harsh conditions.^{59,60} Dual doping has been proven to improve the stability of electrocatalysts. For example, the Mo dopant could enhance the corrosion resistance of Fe/Mo co-doped CoO nanosheet in seawater electrolysis, thereby upgrading the catalyst stability.⁶¹ A central reason for the boosted stability is due to the regulated electronic properties. In a Mo/Ce co-doped RuO_x, the Mo and Ce dopants can transfer electrons to Ru and hinder the dissolution of Ru sites.⁶² Similarly, W/Sn dopants in Ir_{0.7}W_{0.2}Sn_{0.1}O_x can stabilize Ir sites by charge redistribution, limiting the over-oxidation of Ir under high voltages.⁶³ Hao et al. found that W/Er dopants could regulate the electronic property of RuO₂ and prevent the generation of oxygen vacancies, thereby limiting RuO₂ dissolution in acidic electrolyte and achieving high durability over 120 h at 0.1 A cm⁻² in a polymer electrolyte membrane (PEM) electrolyzer.⁶⁴ Dual doping can also benefit stability by regulating the nanostructure of catalysts. In a Mo/S co-doped NiSe₂ catalyst, the Mo and S dopants can boost the stability by forming a porous spongy nanoflake-like structure.⁵⁶ The nanoflake-like nanostructure can promote the gas evolution process and prevent the mechanical destruction/detachment of active sites during electrocatalysis.

3 | CATION–CATION DUAL-DOPED METAL CATALYSTS FOR WATER ELECTROLYSIS

Incorporating two metals into catalysts can activate the catalytic activity and boost the performance. Depending on the properties of metal dopants, a series of cation–cation dual-doped metal oxides, hydroxides, chalcogenides, and pnictides have been designed and used for water electrolysis (Table 1). In this section, recent cation–cation dual-doped metal catalysts are discussed and the dopant-induced performance increase is well explained.

3.1 | Cation–cation dual-doped metal (hydr)oxides

Metal (hydr)oxides are a group of active catalysts for water electrolysis, especially for OER.^{76–78} Nevertheless, the relatively low conductivity and limited active sites hinder their catalytic performance.^{79,80} For activating metal (hydr)oxides, dual cation-doping is suggested to improve the electrical conductivity, introduce new actives, boost intrinsic activity, etc.^{48,81} To improve the catalytic performance of Fe₂O₃, a Ru and Ni dual doping method has been developed by Cui et al.⁶⁶ In their study, a suitable Ru/Ni molar ratio is important for the formation of a lily-like structure, which benefits the exposure of highly active sites. Working as a bifunctional catalyst, the Ru/Ni co-doped Fe₂O₃ demands a cell voltage of 1.73 V to drive 100 mA cm⁻² in the 1 M KOH seawater electrolyte. With good stability for 100 h. Besides nanostructure control, the co-introduction of Ni and Fe could activate the inert W₁₈O₄₉ into an efficient OER catalyst ($\eta_{10} = 325$ mV, Tafel slope = 42 mV dec⁻¹) via enhancing the electrical conductivity, reducing the R_{ct}, populating active sites, introducing oxygen vacancies, and facilitating intermediate adsorption.⁸² Typically, the Fe dopant is suggested to promote the generation of rich Oxygen vacancies, and the Ni dopant can improve the adsorption of OER reactants/intermediates and decrease the reaction energy barrier. Thus, taking advantage of Fe and Ni dopants, the electrochemical activity of W₁₈O₄₉ can be significantly boosted. Ni/Fe dual dopants also have been used to boost the OER performance of an inert MoO₂ catalyst prepared by a hydrothermal method.⁶⁷ In the optimal Mo_{0.9}Ni_{0.05}Fe_{0.05}O₂, the dual dopants can tune the surface chemical environment and the electronic structure of MoO₂ by forming high-valence Mo species (Mo⁶⁺) and hydroxyl-rich surface. Instead of improving the ratio of high-valence metal species, metal dopants (Ni/Co) are suggested to increase the density of active Mn species (Mn³⁺) in a Ni/Co-doped α -MnO₂ nanowire

catalyst.⁸³ Aside from emphasizing the influence of metal dopants on catalytic activities, Liu and coauthors found that the Mo dopant could improve the corrosion resistance of Fe/Mo co-incorporated Co–O nanosheet in seawater electrolysis and thus enhance the stability of the catalyst.⁶¹

Perovskite oxides (ABO₃) are a group of cost-effective OER catalysts with clear active sites. In the ABO₃ structure, cation dopants can be introduced in the A site and/or B site, which leads to diverse doping mechanisms and catalytic performance. Sun et al. developed a Mn/Ni dual-doped LaCoO₃, in which Mn and Ni substitute partial Co sites.³⁹ The dual metal pair doping helps to shift the valence band (O 2p) toward the Fermi level and enhance the covalency of Co–O bonds, thereby improving the OER performance. In the Fe/Sn co-doped BaCoO₃ (BaCo_{0.7}Fe_{0.2}Sn_{0.1}O_{3- δ}), the introduced Fe and Sn dopants at B sites tune the OER intermediate adsorption ability, promote charge transfer capability and electrical conductivity, which therefore increased the OER performance.³⁸ Besides incorporating two metal dopants at B sites, several studies also developed dopants at both A and B sites, such as La_{0.8}Ca_{0.2}Mn_{0.2}Co_{0.8}O₃⁸⁴ and La_{0.4}Sr_{0.6}Ni_{0.5}Fe_{0.5}O₃.⁸⁵ In general, the co-regulation of A and B sites benefits the electronic structure regulation and enhanced electrical conductivity. Dual dopants can also enhance the OER catalytic performance of perovskite oxides by altering the involvement of lattice oxygen for OER. In a Fe/Mn co-doped cobaltate catalyst (La_{0.6}Sr_{0.4}Co_{0.8}Fe_{0.1}Mn_{0.1}O_{3- δ}), the co-incorporation of Fe/Mn elements significantly intensifies the involvement of lattice oxygen for OER and promotes OER kinetics.⁸⁶

RuO₂ and IrO₂ are widely used for acidic OER, and dual cation dopants can further improve their activity and stability. It is suggested that dual metal dopants can activate and stabilize Ru and Ir sites via regulating electronic structures (e.g., work function and *d* band center) of RuO₂ and IrO₂. As shown in Figure 1A, the tiny Pt/La dual-doped IrO₂ nanoparticles dispersed on N-doped carbon (Pt_{0.1}La_{0.1}-IrO₂@NC) were synthesized from a zeolitic imidazolate framework precursor.²⁹ The Pt/La dual-doped catalyst outperforms the mono-doped and undoped counterparts with high stability in the acidic electrolyte (Figure 1B,C). Further DFT calculations implied that the Pt/La dopants optimize the *d*-band center and contribute to the efficient formation of *OOH (potential limiting step), with a lowered energy barrier of 1.66 eV (Figure 1D). Structural stability is a critical issue in the design of acidic OER electrocatalysts. Dual cation dopants have exhibited great potential in enhancing the stability of RuO₂ and IrO₂ by regulating the electronic properties. For example, the Mo/Ce dopants in Ru₃Mo–CeO_x can not only transfer electrons to Ru and limit the

TABLE 1 Representative cation–cation dual-doped metal catalysts for water electrolysis.

Catalyst	Synthetic method	Application	Electrolyte	Performance
Ru/Ni co-doped Co ₃ O ₄ ⁶⁵	Hydrothermal process	OER	1 M KOH	$\eta_{10}^a = 290$ mV, Tafel slope = 76 mV dec ⁻¹
Ru/Ni co-doped Fe ₂ O ₃ ⁶⁶	Hydrothermal process	OER	1 M KOH	$\eta_{100} = 325$ mV, Tafel slope = 60.85 mV dec ⁻¹
		HER	1 M KOH	$\eta_{100} = 75$ mV, Tafel slope = 85.08 mV dec ⁻¹
		OWS	1 M KOH	$E_{100}^b = 1.66$ V
Ni/Fe co-doped MoO ₂ ⁶⁷	Hydrolysis	OER	1 M KOH	$\eta_{10} = 249$ mV, Tafel slope = 58.66 mV dec ⁻¹
Mn/Ni co-doped LaCoO ₃ ³⁹	Hydrothermal process and pyrolysis	OER	0.1 M KOH	$\eta_{10} = 370$ mV
W/Er co-doped RuO ₂ ⁶⁴	Hydrothermal process and calcination	OER	0.5 M H ₂ SO ₄	$\eta_{10} = 168$ mV, Tafel slope = 66.8 mV dec ⁻¹
Pt/La co-doped IrO ₂ ²⁹	Hydrothermal process and pyrolysis	OER	0.5 M H ₂ SO ₄	$\eta_{10} = 205$ mV, Tafel slope = 50.9 mV dec ⁻¹
Mo/Ce co-doped RuO ₂ ⁶²	Pyrolysis	OER	0.5 M H ₂ SO ₄	$\eta_{10} = 164$ mV, Tafel slope = 61.2 mV dec ⁻¹
Ir/Fe co-doped Co (OH) ₂ ⁶⁸	Hydrothermal process	OER	1 M KOH	$\eta_{10} = 254$ mV, Tafel slope = 71.2 mV dec ⁻¹
Cu/Co co-doped Ni ₃ S ₂ ⁶⁹	Hydrothermal process and vulcanization	OER	1 M KOH	$\eta_{100} = 400$ mV, Tafel slope = 94.9 mV dec ⁻¹
Fe/Mn co-doped Ni ₃ S ₂ ⁷⁰	Hydrothermal process and sulfidation	OER	1 M KOH	$\eta_{30} = 216$ mV, Tafel slope = 63.29 mV dec ⁻¹
Cu/Pd co-doped MoS ₂ ⁷¹	Hydrothermal process and chemical reduction	HER	0.5 M H ₂ SO ₄	$\eta_{10} = 93$ mV, Tafel slope = 74 mV dec ⁻¹
		OER	1 M KOH	$\eta_{10} = 248$ mV, Tafel slope = 55 mV dec ⁻¹
		HER	1 M KOH	$\eta_{10} = 63$ mV, Tafel slope = 50 mV dec ⁻¹
Mo/Co co-doped 1T- VS ₂ ⁴⁹	Hydrothermal process	OER	1 M KOH	$\eta_{10} = 248$ mV, Tafel slope = 55 mV dec ⁻¹
		HER	1 M KOH	$\eta_{10} = 63$ mV, Tafel slope = 50 mV dec ⁻¹
		OWS	1 M KOH	$E_{10} = 1.54$ V
Ni/Co co-doped WSe ₂ ⁷²	Hydrothermal process	HER	0.5 M H ₂ SO ₄	$\eta_{10} = 205$ mV, Tafel slope = 118.6 mV dec ⁻¹
Mo/Co co-doped VC ⁷³	Pyrolysis	HER	1 M KOH	$\eta_{10} = 137$ mV, Tafel slope = 93.1 mV dec ⁻¹
Fe/Mn co-doped Ni ₂ P ⁷⁴	Hydrothermal process and phosphorization	OER	1 M KOH	$\eta_{10} = 220$ mV, Tafel slope = 53 mV dec ⁻¹
Ru/Ni co-doped CoP ⁷⁵	Oxidation and phosphorization	OER	1 M KOH	$\eta_{10} = 251$ mV, Tafel slope = 102.3 mV dec ⁻¹
		HER	1 M KOH	$\eta_{10} = 45$ mV, Tafel slope = 53.9 mV dec ⁻¹
		OWS	1 M KOH	$E_{10} = 1.448$ V

Abbreviations: HER, hydrogen evolution reaction; OER, oxygen evolution reaction; OWS, overall water electrolysis.

^a η_{10} : overpotential at the current density of 10 mA cm⁻².

^b E_{100} : applied potential at a current density of 100 mA cm⁻² for overall water electrolysis.

dissolution of Ru sites but also improve the OER performance by enhancing the covalency of Ru–O bonds and the hybridization of *d*–*p* orbitals.⁶² In addition, the W/Sn

dopants in Ir_{0.7}W_{0.2}Sn_{0.1}O_x can stabilize Ir sites via charge redistribution, inhibiting the overoxidation of Ir under high potentials.⁶³ In Hao et al.'s study, W and Er dopants

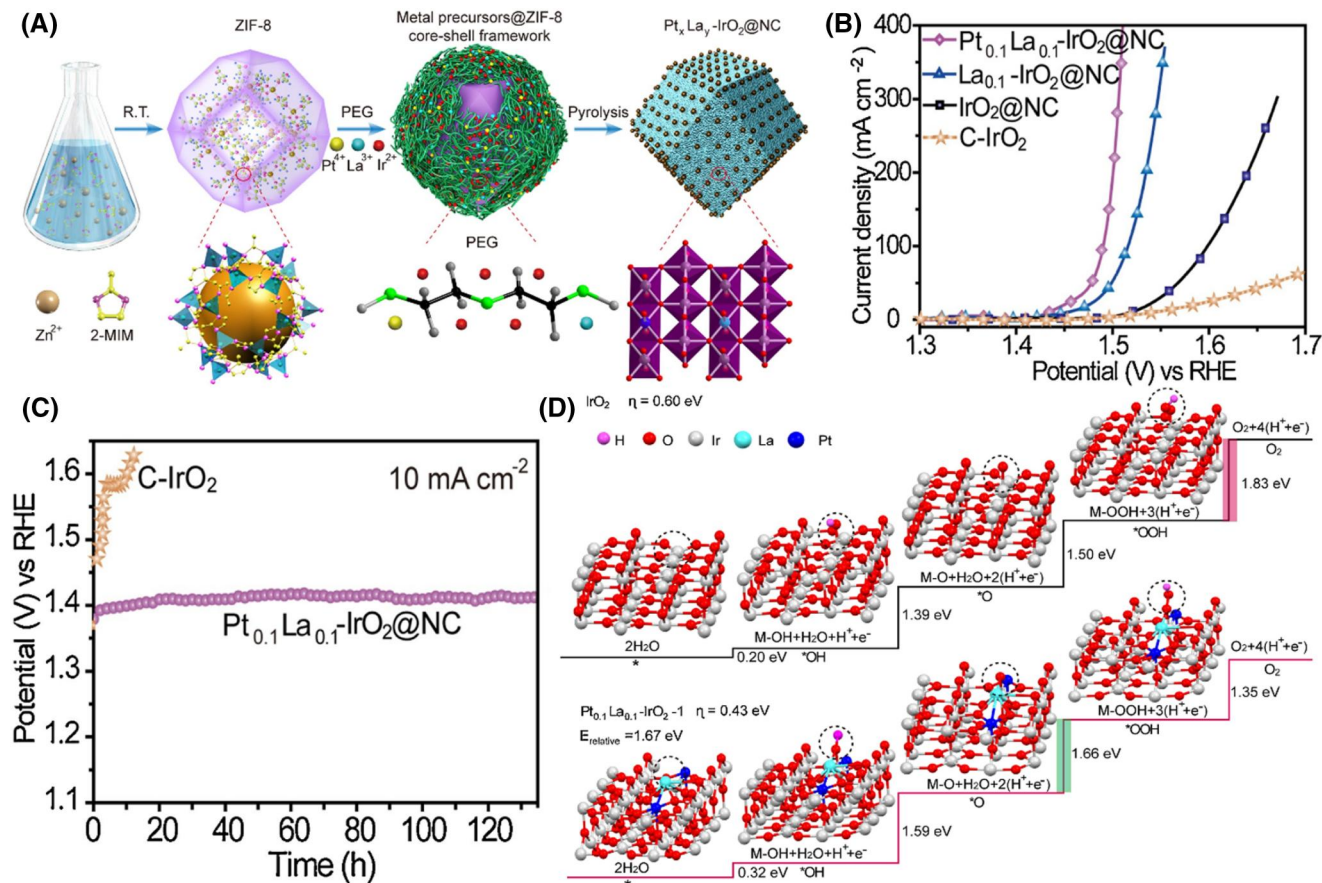


FIGURE 1 (A) Illustration of the synthesis of $\text{Pt}_x\text{La}_y\text{-IrO}_2@\text{NC}$. (B) OER polarization curves of electrocatalysts in 0.5 M H_2SO_4 . (C) Stability curve of $\text{Pt}_x\text{La}_y\text{-IrO}_2@\text{NC}$. (D) Computed energy profiles of IrO_2 and $\text{Pt}_{0.1}\text{La}_{0.1}\text{-IrO}_2$. Reproduced with permission.²⁹ Copyright 2020, Elsevier. OER, oxygen evolution reaction.

can tune the electronic structure of RuO_2 and hinder the formation of oxygen vacancies, which further limit the dissolution of RuO_2 in acidic electrolyte and attain good stability for over 100 h at 0.1 A cm^{-2} in a PEM electrolyzer.⁶⁴

Metal (oxy)hydroxides are recognized as the real active phases of transition metal based OER electrocatalysts.^{87,88} However, the relatively low electrical conductivity and unsatisfied catalytic activities need further improvements. Dual cation doping has been adopted to boost the OER performance of metal (oxy)hydroxides by regulating the electronic properties of host metal sites. In the Nb/Fe dual-doped $\beta\text{-Ni}(\text{OH})_2$ nanosheet, the electronic interaction between Nb, Ni, and Fe benefits the OER process by optimizing Gibbs free energies of OER intermediates.⁸⁹ Moreover, Ir/Fe co-doping can reduce the OER energy barrier over $\text{Co}(\text{OH})_2$ by promoting the formation of the $^*\text{O}$ intermediate.⁶⁸ Similar results that emphasize the role of dual cation dopants in regulating active sites' electronic environments and optimizing the adsorption strength of reaction intermediates have been evidenced by Li et al.⁹⁰ and Wei et al.⁹¹ Of note, the

cation dopants can also work as highly active sites toward OER. For instance, the V site in V/Fe co-doped NiOOH has near-optimal binding energies toward intermediates and shows a lower energy barrier than Ni or Fe sites.⁹²

3.2 | Cation–cation dual-doped metal chalcogenides

Metal chalcogenides (sulfides, selenides, and tellurides) with high conductivity and activity are active materials for both HER and OER.^{93–96} For increasing the active sites and boosting the intrinsic activity of metal chalcogenides, dual cation doping is adopted to alter the electronic structure of catalysts and introduce active sites. Cu/Co co-doped Ni_3S_2 ,⁶⁹ Cu/Fe co-doped Ni_3S_4 ,⁹⁷ Fe/Mn co-doped Ni_3S_2 ,⁷⁰ Co/V co-doped NiS_x ,⁹⁸ Fe/V co-doped Ni_3S_2 ,^{99,100} Fe/Co dual-doped Ni_3S_4 ,¹⁰¹ Co/Mn co-doped $\text{Fe}_9\text{S}_{11}@\text{Ni}_9\text{S}_8$,¹⁰² Fe/Co co-doped Ni_3Se_4 ,¹⁰³ and Ni/Fe co-doped CoSe_2 ,¹⁰⁴ which insert two transition metals into metal chalcogenides are representative of efficient catalysts for water electrolysis. In these catalysts, the

electronic interaction between transition metal dopants and the host metal benefits the optimization of catalysts' electron configuration, thereby decreasing the reaction energy barrier. In addition, the incorporation of transition metal dopants is suggested to improve the electrical conductivity, which also benefits electrochemical reactions.¹⁰⁵ Recently, Krishnamurthy et al. found that Fe and V dopants in Fe/V co-doped Ni₃S₂ led to lattice distortion, and the enrichment of sulfur active edge sites contributed to boosted catalytic performance for OWS.¹⁰⁶ Aside from transition metals, main group metals (e.g., Al) have been used as dopants and some different features have been noticed. In the Fe/Al co-doped NiSe₂, the strong electronic interaction between host Ni sites and Fe/Al dopants helps optimize the adsorption strength of reaction intermediates.¹⁰⁷ In addition, the prominent etching of Al from the catalyst in the alkaline solution leads to rich defective sites and more electroactive sites.

For some typical transition metal dichalcogenides (e.g., VS₂, WS₂, MoS₂, and MoTe₂), the phase structure has a prominent effect on their catalytic performance.^{108–110} Compared with the 2H phase, 1 and 1T' phases are much more active due to the better electrical conductivity.⁴⁹ Cation doping is an efficient approach for realizing the phase transformation of transition metal dichalcogenides.⁷¹ Guided by thermodynamic calculations, Gao and coauthors suggested that co-doping of Co and Ni made it easier to realize the MoTe₂ 2H-to-1T' transformation compared with a series of monometal doping (Figure 2A).⁵⁰ The synergistic effect of Co and Ni largely decreased the energy barrier in the phase transition procedure (Figure 2B). Further analysis indicates that the Ni and Co dopants tune the charge of host Mo atoms by donating 0.118 e⁻ and 0.116 e⁻ to adjacent Mo atoms, respectively (Figure 2C). Compared with the undoped 2H phase MoTe₂, the Co/Ni co-doped 1T' phase MoTe₂ catalysts show significantly improved HER performance (Figure 2D). DFT calculations uncover that Co and Ni dopants can modify the adsorption/desorption strength of H*, and the middle interface of the Co/Ni codoped-MoTe₂ is the most active structure for HER compared with Co and Ni sites (Figure 2E).

3.3 | Cation–cation dual-doped metal pnictides and others

Metal pnictides (nitrides and phosphides) and carbides are extensively used as electrocatalysts for water splitting because of their high electrical conductivity, flexible electronic structures, and good stability.¹¹¹ The intrinsic activity of metal pnictides/carbides can be significantly improved by dual cation doping.^{41,73,112} Generally, the

introduction of cations can regulate catalysts' electronic structures, improve electrical conductivity, and offer additional active sites. In 2022, Liu and coauthors developed a Ni/Mn co-doped FeP with an etching-depositing-phosphorization method.¹¹³ They found that the presence of Ni and Mn dopants can precisely control the *d*-band centers of metal sites, resulting in efficient H* adsorption and *O to *OOH conversion in the HER and OER processes, respectively. Dong et al. also emphasized the role of Co/Ni dopants in tuning the *d*-band structure of the Fe₃N OER catalyst.⁴⁰ The Co/Ni co-doping can induce the lattice expansion and *d*-band center upshift, thereby enhancing the adsorption of *OH and accelerating the generation of active CoNi-FeOOH phase over the surface of Fe₃N. Different from stable dopants such as Ni, Fe, Co, and Mn, introducing sacrificial metal dopants can benefit the introduction of defects and help the exposure of active sites. In a Zn/Fe co-doped CoP catalyst, the Fe dopant not only regulates the nanostructure of CoP and provides rich active sites, but also tunes the electronic properties of CoP and enhances the intrinsic activity.¹¹⁴ In addition, the Zn dopant can increase the catalytic performance by acting as a sacrificial dopant and releasing more electroactive sites during the electrochemical process.

Besides conventional water electrolysis, developing dual cation-doped pnictides for hybrid water electrolysis attracts growing attention owing to the advantage of energy-saving hydrogen production. For instance, Zhai and coauthors designed a Ru/Fe dual-doped Ni₂P catalyst for hydrazine-assisted self-powered hydrogen production.³³ The Ru/Fe co-doped Ni₂P was prepared by a hydrothermal process-phosphorization method (Figure 3A). Compared with undoped and mono-doped Ni₂P, the Ru/Fe co-doped Ni₂P exhibits better performance toward OER and HER (Figure 3B). In addition, adding hydrazine into electrolytes can significantly lower the energy cost for the anode reaction, even in the alkalized seawater electrolyte (Figure 3C). The bifunctional Ru/Fe co-doped Ni₂P only takes 0.69 V to attain 1 A cm⁻² in hydrazine-involved alkalized seawater. Further integrated with a direct hydrazine fuel cell, a self-powered hydrogen production framework has achieved. DFT calculations implied that the co-doped Ni₂P has a thermoneutral hydrogen absorption free energy (ΔG_{H^*}) of -0.13 eV, better than the bare Ni₂P (0.34 eV) (Figure 3D,E). In addition, Fe/Ru dual doping can lower the energy barrier of *N₂H₃ dehydrogenation, enhancing intrinsic dehydrogenation kinetics (Figure 3F). However, as a highly active material for electrooxidation reactions, the involvement of Ru dopant in the hydrazine oxidation process has not been fully discussed.

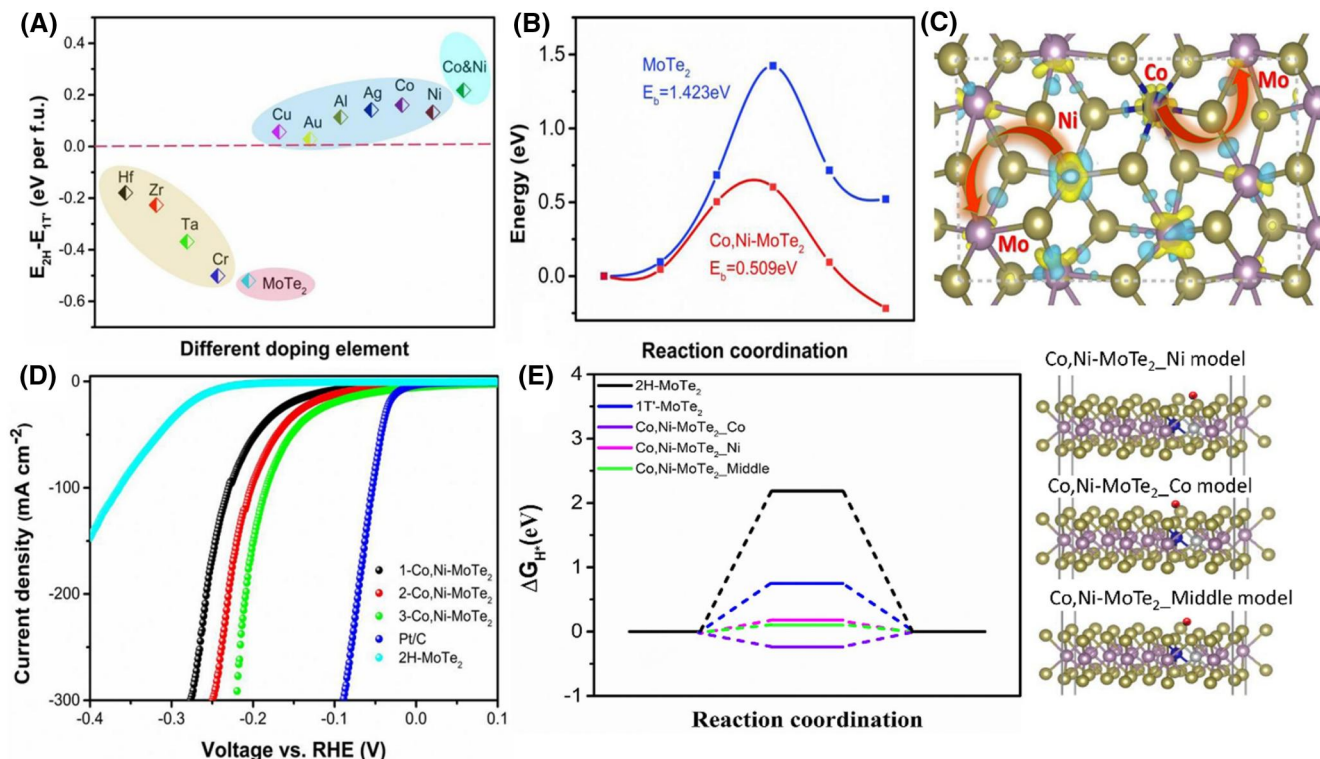


FIGURE 2 (A) The 2H–1T' energy difference for different formula units of MoTe₂ doped with various metals. (B) Reaction coordination-dependent energy profile (phase transition from 2H to 1T') of bare and Co/Ni dual-doped MoTe₂. (C) Charge density difference of Co/Ni dual-doped MoTe₂. (D) HER LSV curves of Co/Ni dual-MoTe₂, Pt/C, and 2H-MoTe₂. (E) Computed energy sketches of 1T'-MoTe₂, Co/Ni dual-doped MoTe₂, and 2H-MoTe₂. Reproduced with permission.⁵⁰ Copyright 2022, Elsevier. HER, hydrogen evolution reaction; LSV, linear sweep voltammetry.

4 | CATION–ANION DUAL-DOPED METAL CATALYSTS FOR WATER ELECTROLYSIS

Cation–anion dual doping is widely used to enhance metal catalysts' performance by regulating the internal and external characteristics (e.g., morphology, electronic structure). With significantly different electronegativities, cation–anion co-doping is capable of tuning the electronic properties of metal catalytic within a wider range than cation–cation doping or anion–anion doping. To date, dozens of cation–anion dual-doped metal catalysts have been designed for water electrolysis, such as metal (hydr)oxides, chalcogenides, pnictides, borides, carbides, and metal particles (Table 2).

4.1 | Cation–anion dual-doped metal (hydr)oxides

The application of metal (hydr)oxides in water electrolysis is hindered by their relatively low electrical conductivity and mediocre intrinsic activity.^{129–131} The collaborative effect of cation and anion dopants augments

the catalytic performance of metal (hydr)oxides by regulating their electronic and geometric structures, enhancing the conductivity, providing active sites, etc.^{54,55,132,133} For example, the Mn dopant can alter the electronic property of Co sites in a metal–organic framework (MOF)-derived Co₃O₄ catalyst, while S dopant helps to increase electrical conductivity and offers active S sites toward the proton adsorption step.⁵³ Therefore, S and Mn co-doping benefits the catalytic performance of Co₃O₄. Zhang et al. found that the Fe and P dopants in Fe/P co-doped NiMoO₄ could enhance the adsorption strength of the H₂O molecule and promote the OER process.¹³⁴ In general, synergistic regulation of cation and anion dopants with opposite electron density states can finely moderate the electronic properties of metal (hydr)oxides, leading to favorable intrinsic activity.^{135–137} Interestingly, the incorporated dopants can work as active sites for water electrolysis. In Ru/P co-doped NiMoO₄ nanorods fabricated via a hydrothermal process-phosphorization method (Figure 4A,B), Ru and P dopants can jointly tune the *d*-band center of NiMoO₄ and also contribute to enhanced catalytic performance by providing additional active sites.³¹ Compared with P-doped and undoped NiMoO₄, the Ru/P co-doped

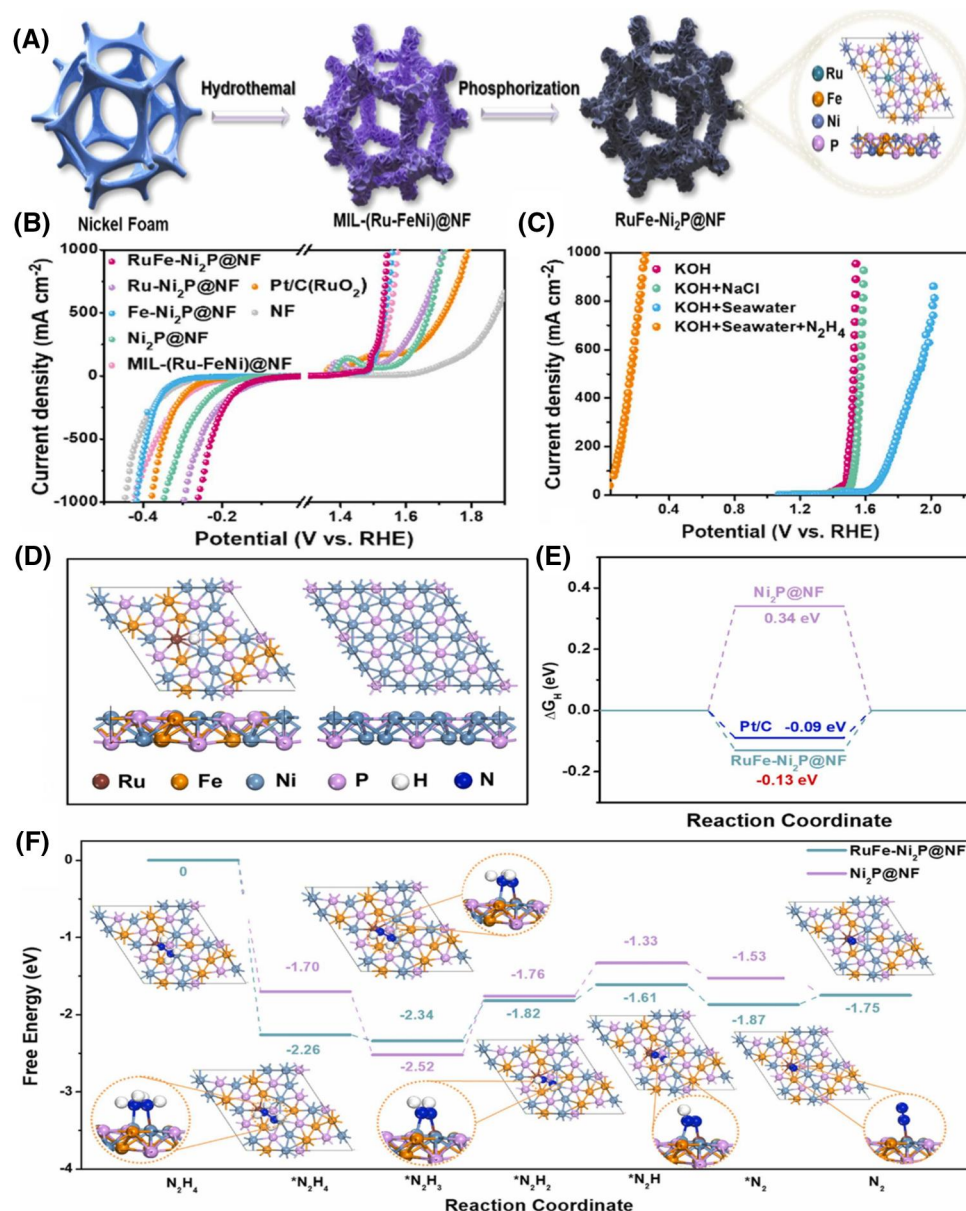


FIGURE 3 (A) Scheme of the preparation of RuFe-Ni₂P@NF. (B) OER and HER LSV curves of electrocatalysts. (C) N₂H₄ oxidation reaction LSV curves of RuFe-Ni₂P@NF in various electrolytes. (D) Structure models of Ni₂P and RuFe-Ni₂P. (E) HER free-energy profiles for Pt/C, Ni₂P, and RuFe-Ni₂P. (F) Free energy diagrams for N₂H₄ oxidation over Ni₂P and RuFe-Ni₂P. Reproduced with permission.³³ Copyright 2023, Elsevier. HER, hydrogen evolution reaction; LSV, linear sweep voltammetry; OER, oxygen evolution reaction.

NiMoO₄ exhibits significantly improved activities toward OER ($\eta_{100} = 281$ mV, Tafel slope = 160.6 mV dec⁻¹), HER ($\eta_{100} = 47$ mV, Tafel slope = 50.1 mV dec⁻¹), as well as urea oxidation reaction in seawater (Figure 4C,D). Further analysis finds that dual doping of P and Ru increases electrons at the Ru dopant site, which benefits reactant activation and enhances reaction intermediate adsorption (Figure 4E,F). By analyzing the electron localization property of P and Ru dopants, it can be seen that the Ru dopant is bonded with O and P and the Ru-O coordination environment is regulated in the presence of P dopant, indicating that more charges would participate

in electrocatalytic reactions over Ru/P co-doped NiMoO₄ (Figure 4G,H). The Ru and P co-doping also leads to a lower work function of 6.554 eV than their counterparts, confirming the facile electron migration in the Ru/P-NiMoO₄ and thereby accelerating the catalytic reaction (Figure 4I). The density of states (DOS) of Ru/P-NiMoO₄ suggest a metallic feature, which is conducive to electrochemical reactions. Compared with undoped and single-doped NiMoO₄, Ru/P-NiMoO₄ shows a higher *d*-band center of -2.176 eV, which promotes the adsorption of reactants (Figure 4J). Additionally, the DOS of Ru/P-NiMoO₄ at the Fermi level is largely increased with Ru/P

TABLE 2 Representative cation–anion dual-doped metal catalysts for water electrolysis.

Catalyst	Synthetic method	Application	Electrolyte	Performance
Nb/P co-doped NiFe ₂ O ₄ ¹¹⁵	Hydrothermal process and phosphorization	OER	1 M KOH	$\eta_{100} = 247$ mV, Tafel slope = 54.12 mV dec ⁻¹
		HER	1 M KOH	$\eta_{100} = 127$ mV, Tafel slope = 28.1 mV dec ⁻¹
		OWS	1 M KOH	$E_{10} = 1.56$ V
Co/N co-doped MoO ₂ ¹¹⁶	Hydrothermal process and pyrolysis	HER	0.1 M KOH	$\eta_{100} = 258$ mV, Tafel slope = 126.8 mV dec ⁻¹
Mo/P co-doped ZnCo-LDH ¹¹⁷	Hydrothermal process	OER	1 M KOH	$\eta_{50} = 300.1$ mV, Tafel slope = 89.8 mV dec ⁻¹
		HER	1 M KOH	$\eta_{10} = 161.7$ mV, Tafel slope = 61.1 mV dec ⁻¹
		OWS	1 M KOH	$E_{50} = 1.56$ V
Co/B co-doped Ni ₃ S ₄ ¹¹⁸	Electrodeposition	HER	1 M KOH	$\eta_{10} = 35$ mV, Tafel slope = 52 mV dec ⁻¹
Mn/N co-doped Co ₉ S ₈ ¹¹⁹	Hydrothermal process and nitridation	HER	1 M KOH	$\eta_{10} = 102$ mV, Tafel slope = 107.2 mV dec ⁻¹
Mo/S co-doped NiSe ₂ ⁵⁶	Electrodeposition	HER	1 M KOH	$\eta_{10} = 89$ mV, Tafel slope = 57 mV dec ⁻¹
Ru/O co-doped MoS ₂ ¹²⁰	Hydrothermal process	HER	1 M KOH	$\eta_{10} = 43$ mV, Tafel slope = 63.1 mV dec ⁻¹
Co/P co-doped VN ¹²¹	Hydrothermal process and annealing	OER	1 M KOH	$\eta_{10} = 335$ mV
		HER	1 M KOH	$\eta_{10} = 137$ mV, Tafel slope = 81 mV dec ⁻¹
		OWS	1 M KOH	$E_{10} = 1.70$ V
Fe/O co-doped Ni ₂ P ¹²²	Hydrothermal process and phosphorization	OER	1 M KOH	$\eta_{10} = 210$ mV, Tafel slope = 48 mV dec ⁻¹
Zn/F co-doped NiCoP ¹²³	Hydrothermal process and phosphorization	OER	1 M KOH	$\eta_{50} = 285$ mV, Tafel slope = 78.33 mV dec ⁻¹
		HER	1 M KOH	$\eta_{10} = 59$ mV, Tafel slope = 81.03 mV dec ⁻¹
		OWS	1 M KOH	$E_{10} = 1.568$ V
Ru/S co-doped Ni ₂ P ¹²⁴	Hydrothermal method, immersion, and annealing	HER	1 M KOH	$\eta_{10} = 49$ mV, Tafel slope = 43.1 mV dec ⁻¹
Mn/N co-doped Mo ₂ C ¹²⁵	Pyrolysis	HER	0.5 M H ₂ SO ₄	$\eta_{10} = 163$ mV, Tafel slope = 66 mV dec ⁻¹
Ni/P co-doped Mo ₂ C ¹²⁶	Annealing	HER	1 M KOH	$\eta_{10} = 209$ mV, Tafel slope = 39.87 mV dec ⁻¹
W/P co-doped FeB ¹²⁷	Chemical reduction	OER	1 M KOH	$\eta_{10} = 199$ mV, Tafel slope = 39.87 mV dec ⁻¹
Ni/P co-doped Rh ¹²⁸	Chemical reduction	HER	0.5 M H ₂ SO ₄	$\eta_{10} = 15$ mV, Tafel slope = 29 mV dec ⁻¹
		HER	1 M KOH	$\eta_{10} = 36$ mV, Tafel slope = 38 mV dec ⁻¹
		HER	1 M PBS	$\eta_{10} = 44$ mV, Tafel slope = 88 mV dec ⁻¹

Abbreviations: HER, hydrogen evolution reaction; OER, oxygen evolution reaction; OWS, overall water electrolysis; PBS, phosphate buffer solution.

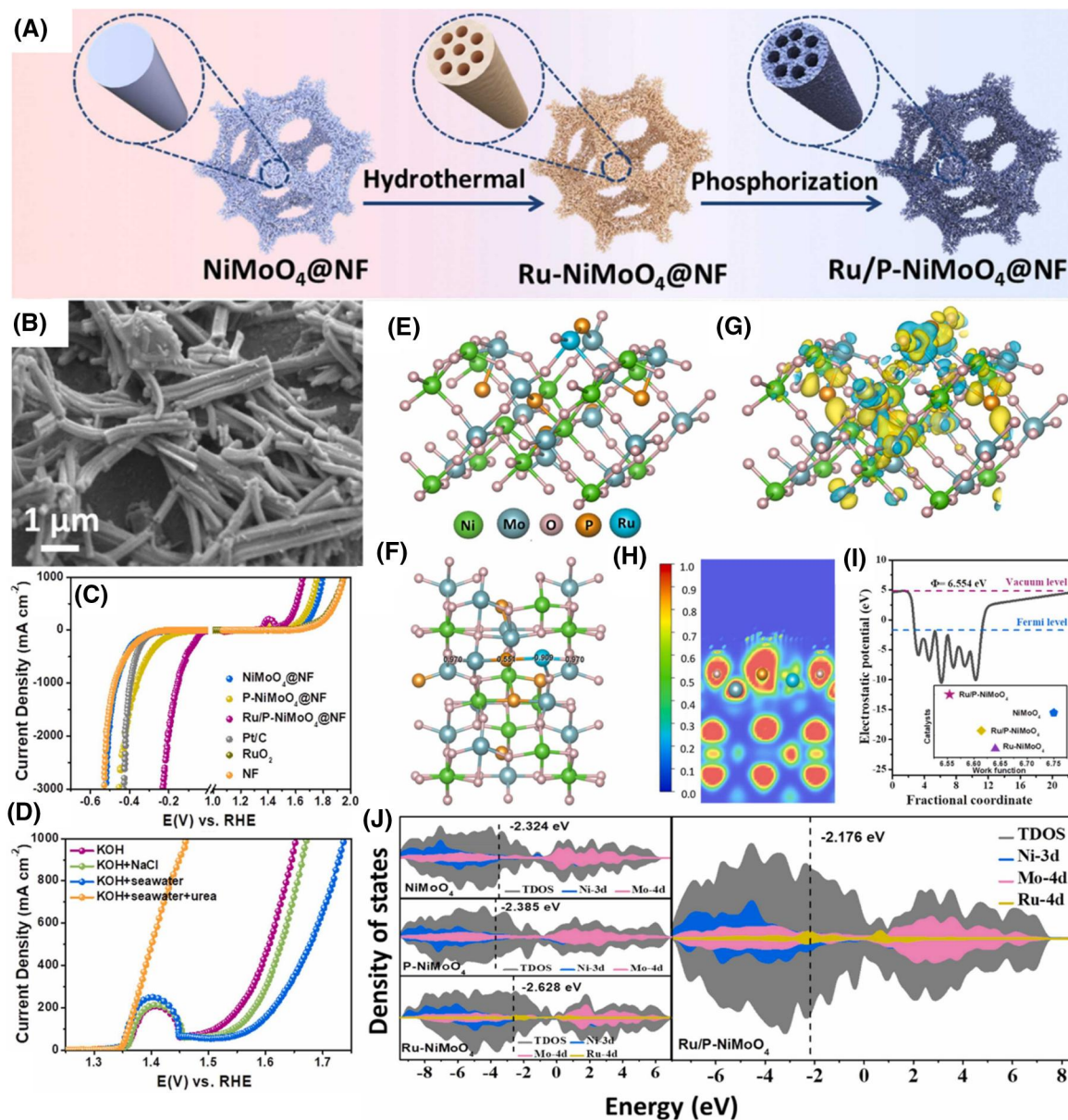


FIGURE 4 (A) Illustration of the synthesis of Ru/P-NiMoO₄@NF. (B) SEM image of Ru/P-NiMoO₄@NF. (C) Polarization curves of HER and OER. (D) LSV curves of Ru/P-NiMoO₄@NF for OWS in KOH, simulated seawater, seawater, and urea-containing seawater. (E) Crystal structure of Ru/P-NiMoO₄. (F) Bader charge and (G) charge density of Ru/P-NiMoO₄. (H) ELF of Ru/P-NiMoO₄ (220) plane. (I) Work function of Ru/P-NiMoO₄. (J) DOS of P-NiMoO₄, Ru/P-NiMoO₄, Ru-NiMoO₄, and NiMoO₄. Reproduced with permission.³¹ Copyright 2023, Elsevier. DOS, density of states; ELF, electron localization function; HER, hydrogen evolution reaction; LSV, linear sweep voltammetry; SEM, scanning electron microscopy; OER, oxygen evolution reaction; OWS, overall water electrolysis.

dual doping and the electrons of Ru account for a big proportion of the DOS near the Fermi level, suggesting that electrons of Ru are active for electrocatalytic reactions, thereby enhancing its catalytic activity.

Oxygen vacancies are important for raising the catalytic performance of metal (hydr)oxides via regulating the electronic structure and increasing active sites. Recent studies suggest that cation–anion dual doping can introduce oxygen vacancies into the crystal structure of metal (hydr)oxides. In the Fe/borate co-doped NiO, the borate

doping induces rich oxygen vacancies.¹³⁸ With a low-coordination number, oxygen vacancies in the NiO₆ structure could be activated by the surrounding delocalized electrons for optimizing the intermediate adsorption strength in OER. Wang et al. found that oxygen vacancies in N/Mn dual-doped Co₃O₄ could not only tune the adsorption strength of OER intermediates and decrease the energy barrier of the rate-determining step but also enhance the electrical conductivity.⁴⁵ Together with a hierarchical structure and rich active

sites, the N/Mn co-doped Co_3O_4 can attain 100 mA cm^{-2} at a low η of 320 mV and a good durability for 40 h.

The nanostructure of catalysts largely governs the active surface area and exposed active sites. Apart from regulating synthetic parameters, such as reaction time and temperature, using dopants can also control the nanostructure of catalysts. For example, the Mo/P dual doping benefits the formation of nanosheet array structures, and the dopants also modify the surface electronic states of Ni-Co-O.⁵⁵ Li and coauthors suggested that Cr doping could modify the nanorods morphology of Cr/P co-doped NiMoO_4 and expose more active sites, and P dopant could significantly boost chemical and mechanical stability as well as HER kinetics.¹³⁹ In Li et al.'s study, the Fe-doped NiMoO_4 shows a disordered structure composed of microsheets and microrods, while the S/Fe co-doped NiMoO_4 can further promote the growth of nanostructure and forms a nanorod array.⁵⁴ The open array benefits the exposure of active sites, charge/mass transfer, and gaseous product release process during OER. It is worth noting that the superhydrophilic/superaerophobic properties are important for gas-involved catalytic reactions. A superhydrophilic surface can improve the catalyst wettability and promote the adsorption of reactants (e.g., H_2O), and a super-aerophobic surface can accelerate bubble release in the catalytic process. By doping with P and Nb, the P, Nb- NiFe_2O_4 catalyst with a nanosheet structure shows superhydrophilic and superaerophobic characteristics, which would offer critical kinetic advantages for enhancing reaction efficiency and gas generation rate.¹¹⁵

4.2 | Cation–anion dual-doped metal chalcogenides

Compared with metal (hydr)oxides, metal chalcogenides with higher electrical conductivity are attractive electrocatalysts for water splitting.^{95,140–142} Cation–anion dual doping has been widely applied for improving the catalytic performance of Ni sulfides/selenides, Co sulfides/selenides, and MoS_2 -type layered metal disulfides. In general, cation and anion dopants can enhance the intrinsic activity of Ni/Co chalcogenides by regulating their electronic properties.^{119,143–146} As reported, cation and anion dopants can shift metals' *d*-band center, which affects the adsorption/desorption strength of reactants/intermediates and contributes to promoted catalytic performance.^{118,147} Since high-valence metal sites are highly active toward OER, introducing cation dopants with a high valence is suggested. In an N/Ce co-doped CoS_2 catalyst, the N and Ce dual dopants synergistically stabilize the OER intermediates and accelerate the catalysis

process by forming two high oxidation state active metal sites.¹⁴⁸ Cr is another widely used metal dopant with a high oxidation state. Chen et al. developed a Cr/P co-doped Co_3S_4 catalyst (Cr, P- Co_3S_4) with a hydrothermal treatment-phosphorization process.¹⁴⁹ As shown in Figure 5A, the incorporation of Cr and P dopants regulates the charge of nearby Co and S atoms and leads to charge redistribution within the lattice. Compared with the single Cr or P doped Co_3S_4 , the dual doping process shows a more negative formation energy (Figure 5B), indicating the spontaneous formation and stable existence of the Cr, P- Co_3S_4 catalyst. In addition, the *d*-band center of Co in Cr, P- Co_3S_4 is lower than that in bare Co_3S_4 , which weakens the interaction between OER intermediates and Co sites and balances the adsorption/desorption of intermediates (Figure 5C). This is further evidenced by the free energy diagrams in Figure 5D, where the energy barrier for *OOH formation over Cr, P- Co_3S_4 is lower than that for Co_3S_4 (2.30 vs. 2.39 eV). The electrochemical tests confirm the higher OER activity and stability of Cr, P- Co_3S_4 than its counterparts (Figure 5E,F).

Dopant-induced lattice distortion is effective for boosting the intrinsic activity of Ni/Co chalcogenides by introducing rich highly active defective sites. With high-resolution transmission electron microscopy (HRTEM) images, Jiang et al. found that the lattice fringes of Cu/F co-doped CoS were discontinuous and the presence of Cu and F dopants lead to abundant vacancies and disordered constructions on crystal planes of the catalyst.¹⁵⁰ The lattice distortion can introduce various active defects and edge sites, which helps to optimize the intermediate adsorption capability and improve the electrical conductivity. Working as the bifunctional catalyst for OWS, Cu/F co-doped CoS takes a lower potential of 1.52 V at 10 mA cm^{-2} than F-doped CoS (1.64 V), Cu-doped CoS (1.69 V), and pristine CoS (1.88 V). Although Wang and coauthors declared that the P and Cu dopants could enhance the catalytic performance of $\text{Co}_{0.85}\text{Se}$ by contorting the lattice,¹⁵¹ there was no clear evidence to support the regulated lattice structure.

Apart from focusing on the positive effect of cation–anion dual dopants on the catalytic activities of catalysts, some studies have uncovered the contribution of cation–anion co-doping on catalysts' stability. For sustainable seawater electrolysis, Chang and coworkers designed a Fe/P co-doped NiSe_2 catalyst.³² The P dopant enhances the electrical conductivity and protects selenide from dissolution via forming a P–O species passivation layer. Similarly, the P dopant in the Fe/P co-doped CoS_2 catalyst also helps to improve the mechanical and chemical stability.¹⁵² In Mo/S co-doped NiSe_2 , Mo and S dopants can boost stability by forming a porous spongy

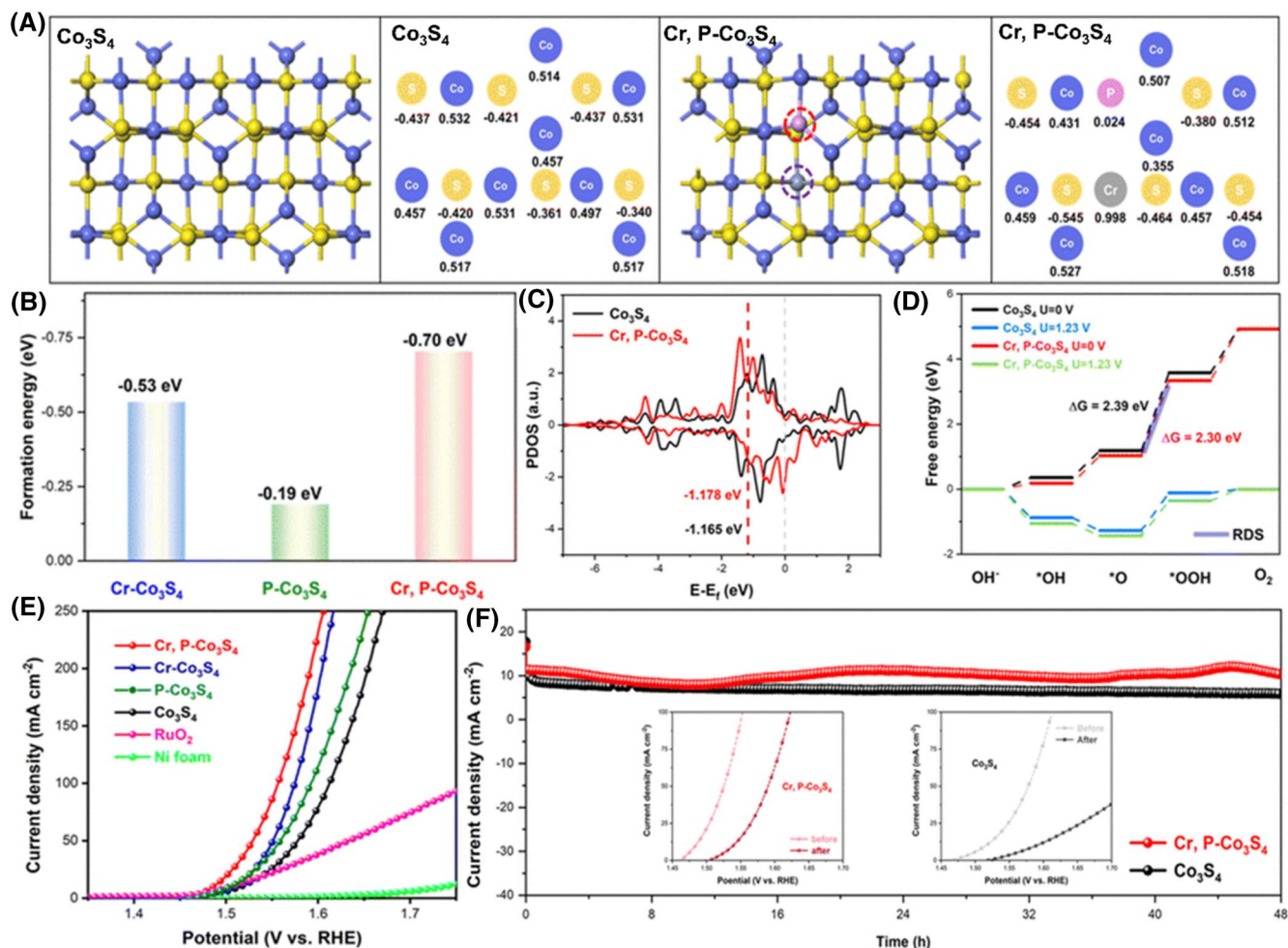


FIGURE 5 (A) Crystal structures and atom charges of Cr, P-Co₃S₄ and Co₃S₄ (P: purple, Cr: gray, S: yellow, and Co: blue). (B) Formation energies of P-Co₃S₄, Cr, P-Co₃S₄, and Cr-Co₃S₄. (C) DOS of Co 3d bands of Cr, P-Co₃S₄ and Co₃S₄. (D) OER free-energy profiles of Cr, P-Co₃S₄ and Co₃S₄. (E) OER LSV curves of electrocatalysts. (F) *I*-*t* curves of Co₃S₄ and Cr, P-Co₃S₄ at ~10 mA cm⁻², inserts show LSV curves of Cr, P-Co₃S₄ and Co₃S₄ before and after the stability test. Reproduced with permission.¹⁴⁹ Copyright 2023, Royal Society of Chemistry. DOS, density of states; LSV, linear sweep voltammetry; OER, oxygen evolution reaction.

nanoflake-like structure.⁵⁶ The nanostructured catalyst can facilitate the gas evolution process and avoid the mechanical destruction of active sites during HER.

Layered metal disulfides (e.g., MoS₂ and WS₂) are promising noble-metal-free materials for HER. Nevertheless, active sites of WS₂ and MoS₂ are mainly located at their edges, while main basal planes are catalytically inert.¹²⁰ Cation-anion dual doping is capable of activating MoS₂ and WS₂. Guided by computational studies, Co/X (X = Se, C, and N) dual dopants are suggested to enhance the HER performance of the MoS₂ monolayer by leading to near-zero Δ*G*_{H*} at moderate compressive or extensile strain.¹⁵³ Similarly, Co and N dual dopants are suggested to boost the HER activity of WS₂ via enhancing the hydrogen adsorption ability and reducing the energy barriers for H₂O adsorption and dissociation. The Co/N co-doped WS₂ attains 10 mA cm⁻² at an η of 132 mV,

which is significantly smaller than N doped WS₂ (376 mV) and WS₂ (417 mV).¹⁵⁴ Cao et al. found that Co/O dopants could form in-plane Co-O-Mo species in 1T phase MoS₂ structure, thus accelerating the water dissociation process.¹⁵⁵ It should be noted that the cation-anion dual doping can introduce defect pairs into the basal plane of MoS₂, resulting in highly active sites. In a Pd/O co-doped MoS₂, the Pd and O defect pairs together with unsaturated S atoms can promote the intrinsic activity toward HER.¹⁵⁶

4.3 | Cation-anion dual-doped metal pnictides

Cation-anion co-doping is capable of altering the properties of metal pnictides and contributes to improved

catalytic performance. In general, the cation and anion dopants can tune the electronic properties (e.g., *d* band center and charge distribution) of metal pnictides,¹⁵⁷ which enhances catalysts' intrinsic activity via optimizing the adsorption/desorption of reactants/intermediates.^{124,158–160} For instance, Zhao and coworkers designed a B/V co-doped Ni₂P catalyst (B, V-Ni₂P) with a three-step method (Figure 6A).¹⁶¹ The B, V-Ni₂P has a nanosheet structure (Figure 6B), with the formation of amorphous regions (Figure 6C). The amorphous/crystalline structure has been proven to be active for catalytic reactions. DFT calculations indicate that the introduction of B and V dopants results in a lower *d*-band center than bare Ni₂P (Figure 6D,E), suggesting that dual dopants help to weaken the adsorption of H*. In addition, B/V dopants facilitate water dissociation and balance the H* adsorption and H₂ desorption during alkaline HER (Figure 6F,G). Thus, B, V-Ni₂P shows high HER activities

in alkalized seawater ($\eta_{10} = 74$ mV), and it also works well as a cathode in two-electrode seawater splitting (Figure 6H,I). Similar studies also illustrate that cation-anion dual dopants can optimize the electronic configuration of metal pnictides and induce lattice irregularity, thereby improving the intrinsic activity.^{18,44,162}

Metal sites with high oxidation states are active toward OER,^{163,164} and using suitable dopants to keep metal species at high valences is an efficient method. In a Co/N co-doped Ni₂P, the Co and N dopants with different electron affinities not only tune the surface electronic structure but also form diverse electroactive sites with high valence states.¹⁶⁵ With X-ray photoelectron spectroscopy (XPS) analyses, Bo et al. found that the strong coupling interaction in the Fe/O co-doped Ni₂P could regulate electronic properties, resulting in relatively higher oxidation states and stronger oxidation ability of the catalyst.¹²² At 10 mA cm⁻², a low η of 210 mV is

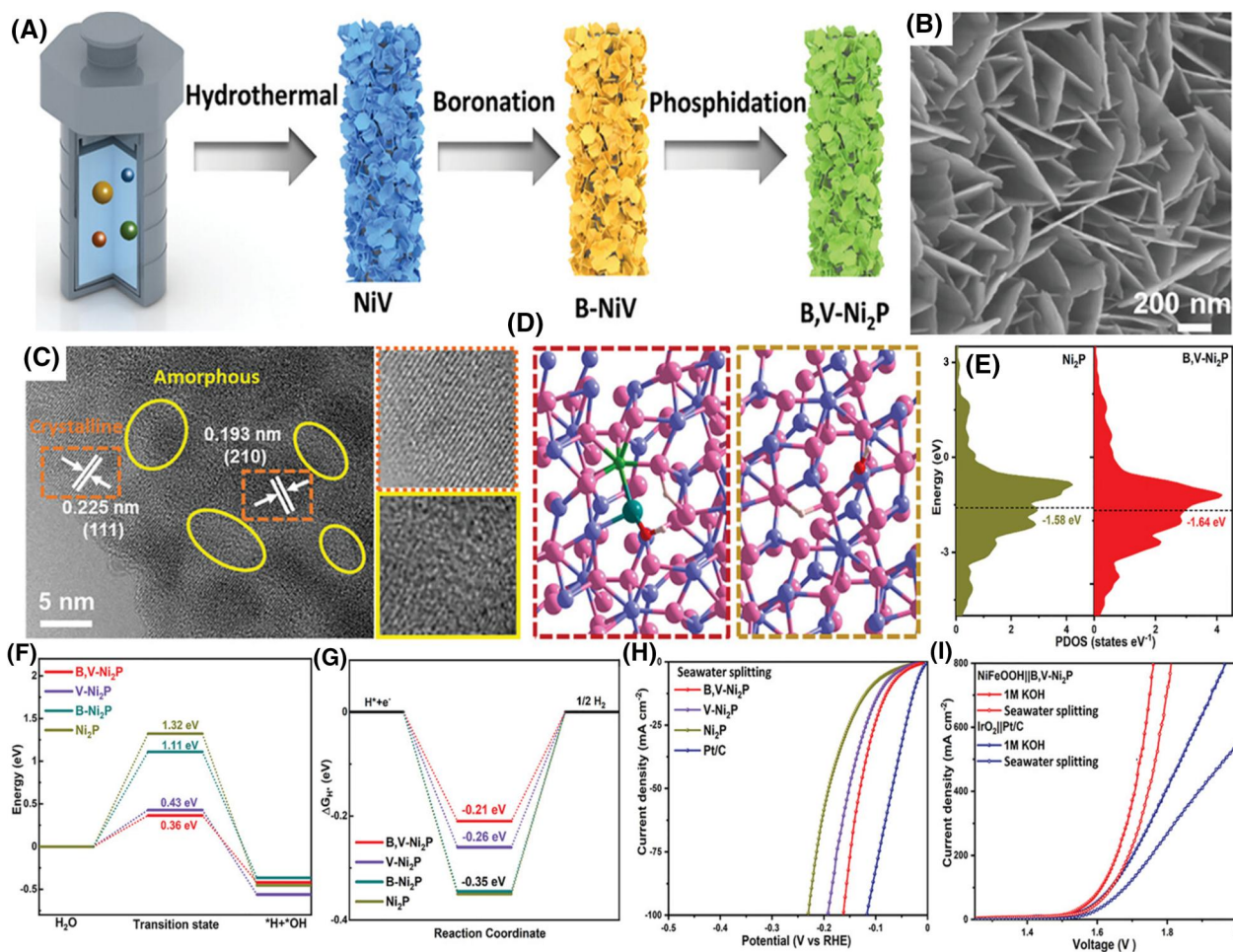


FIGURE 6 (A) Illustration of the fabrication of B, V-Ni₂P. (B) SEM and (C) TEM images of B, V-Ni₂P. (D) Adsorption models of OH* and H* on B, V-Ni₂P and Ni₂P, respectively. (E) DOS of Ni atoms for Ni₂P and B, V-Ni₂P. Free-energy profiles for (F) H₂O dissociation and (G) H adsorption for B, V-Ni₂P, and analogs. (H) HER LSV curves of catalysts. (I) Polarization curves for water electrolysis in 1 M KOH and seawater over IrO₂||Pt/C and NiFeOOH||B, V-Ni₂P. Reproduced with permission.¹⁶¹ Copyright 2023, Wiley. DOS, density of states; HER, hydrogen evolution reaction; LSV, linear sweep voltammetry; SEM, scanning electron microscopy; TEM, transmission electron microscopy.

needed over the Fe/O co-doped Ni₂P catalyst. Although XPS spectra can help to illustrate the chemical states of elements, an accurate surface chemistry analysis with X-ray absorption spectroscopy is more sensible for identifying high-valence states of the metals.

Cation–anion dual dopants can affect the evolution of active phases by controlling the structure reconstruction of metal pnictides.¹⁶⁶ For OER, Luo and coauthors noticed that the S dopant in Ni/S co-doped CoP₃ could accelerate the surface reconstruction and promote the generation of active CoOOH phase, and Ni dopant enhanced the OER activity and selectivity via electronic regulation.¹⁶⁷ However, the possible role of the P anion in influencing the surface reconstruction was ignored. In a metal (Mn or Fe) and S co-doped MoP HER catalyst, the oxophilic Fe or Mn on the catalyst surface can form Fe or Mn oxide/hydroxide phases during HER, which promotes the water dissociation process in alkaline electrolyte.¹⁶⁸ Such in situ structure reconstruction phenomena are well demonstrated in different metal pnictide-based catalysts, while it remains challenging to identify the role of cation and anion dopants due to the high complexity of chemical composition and structure of cation–anion dual-doped catalysts.

4.4 | Cation–anion dual-doped metals, metal carbides/borides

Metal nanostructures, metal carbides, and borides have a metallic nature, endowing them with high electrical conductivity. Cation–anion dual doping is effective in enhancing the catalytic performance of these materials by populating active sites, regulating electronic properties, inducing lattice strain, etc.¹²⁸ In 2020, Hoa et al. employed a hydrothermal treatment-thermal reduction-electrodeposition method to fabricate a composite catalyst consisting of Mo/P co-doped Co layers on Co nanowires (Co-Mo-P/CoNWs) (Figure 7A).¹⁶⁹ Co-Mo-P/CoNWs has an open structure with abundant disordered wrinkles on the surface (Figure 7B,C), benefiting the exposure of electroactive sites and charge/mass transport during electrocatalysis. Compared with the mono-doped catalysts, Co-Mo-P/CoNWs has a higher proportion of electronic states around the Fermi level, suggesting fast electron transfer and better reactivity (Figure 7D). In addition, the ΔG_{H^*} values on Co, Mo, and P sites in Co-Mo-P/CoNWs indicate an enhanced HER activity than the Co-Mo and Co-P systems (Figure 7E). Experimental results evidence the beneficial role of the dual Mo and P dopants in enhancing the HER and OER performance. In the two-electrode electrolysis system, bifunctional Co-Mo-P/CoNWs outperform the precious metal-based Pt/

ClRuO₂/C electrodes at 100 mA cm⁻² (Figure 7F,G), with high Faradic efficiencies for H₂ (98.2%) and O₂ (98.45%) (Figure 7H). In this study, the Mo and P dopants improve the catalytic performance mainly by jointly regulating the electronic property of Co, which is different from the activation mechanism of the Co/S co-doped Ni catalyst. In Co/S co-doped Ni, the S dopant induces electron localization at adjacent Co and Ni atoms, while the Co dopant works as the reactive sites for the Volmer step of HER.¹⁷⁰ It has also been suggested that Ni and P dopants can induce lattice strain in Rh, and the electronic interaction between Ni, P, and Rh can precisely alter the electronic properties of Rh atoms and weaken hydrogen binding strength, thus promoting the HER performance.¹²⁸

With a similar electronic structure to that of Pt, metallic Mo₂C is a promising HER catalyst. Recently, Mn/N,¹²⁵ P/Ni,¹²⁶ Zn/N,¹⁷¹ and Ni/N¹⁷² have been developed as dual dopants for activating Mo₂C. In these reports, the cation and anion dopants are suggested to synergistically adjust the electronic structure of Mo₂C and optimize ΔG_{H^*} values, thereby enhancing intrinsic activity. Additionally, Zhou and coauthors found that the incorporated Mn dopant could work as active sites toward HER.¹²⁵ Amorphous metal borides are a group of highly active catalysts for water electrolysis.^{173–177} Chen and coauthors developed a W/P dual-doped FeB for OER,¹²⁷ in which the electrochemical etching of P and B anions promoted the surface reconstruction of FeB and accelerated the formation of FeOOH. In addition, The W dopant enhances the OER activity of self-evolved FeOOH by enhancing the conductivity and regulating the adsorption strength of OER intermediates. In 1 M KOH, W/P co-doped FeB needs 199 mV at 10 mA cm⁻². This study emphasizes the role of dopants in the structure reconstruction process of catalysts, which provides insights into the design of efficient transitional metal-based catalysts.

5 | ANION–ANION DUAL-DOPED METAL CATALYSTS FOR WATER ELECTROLYSIS

Anion dopants (e.g., S, P, N, B, Se, Te, F, and Cl) with relatively high electronegativities are generally used to regulate the electronic structure of electrocatalysts,^{178–181} in addition to their key role in accelerating structure reconstruction (especially during OER).^{182–186} Compared with mono-doping, dual-anion doping can help to precisely tailor the electronic properties of metal catalysts and boost the catalytic performance. To date, a series of anion–anion dual-doped metal catalysts have been

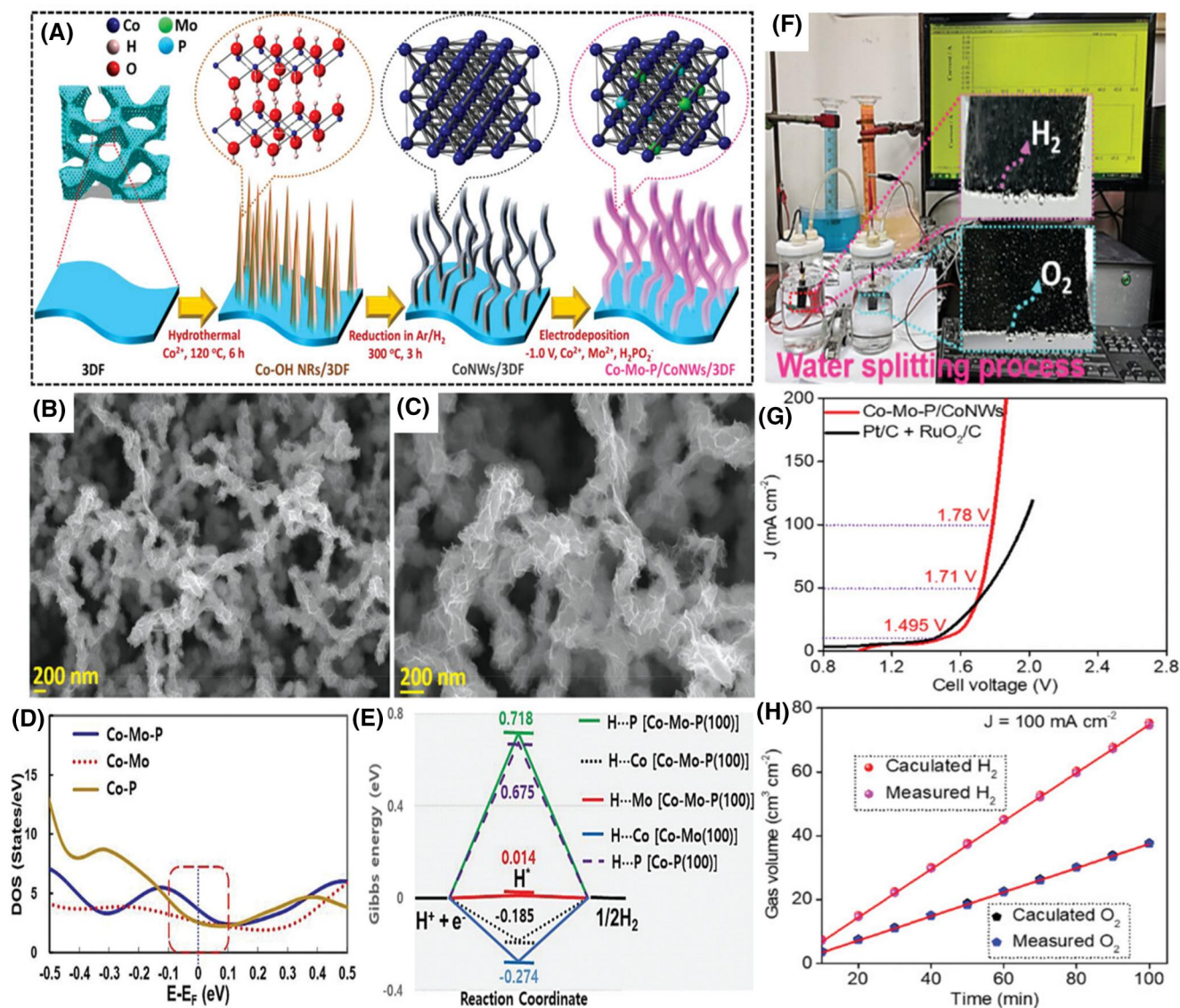


FIGURE 7 (A) Scheme of the fabrication of Co-Mo-P/CoNWs. (B and C) SEM images of Co-Mo-P/CoNWs. (D) DOS and (E) ΔG_{H^+} for different catalysts. (F) Photograph of the water electrolysis process. (G) LSV curves for water electrolysis over Pt/C||RuO₂/C electrodes and bifunctional Co-Mo-P/CoNWs. (H) Calculated and measured gas volumes of the Co-Mo-P/CoNWs-involved electrolyzer. Reproduced with permission.¹⁶⁹ Copyright 2020, Wiley. DOS, density of states; LSV, linear sweep voltammetry; SEM, scanning electron microscopy.

designed for water electrolysis (Table 3), including metal (hydr)oxides, chalcogenides, pnictides, alloys, MOFs, etc.

5.1 | Anion–anion dual-doped metal (hydr)oxides

Ni/Co/Fe-based (hydr)oxides are extensively investigated catalysts for water electrolysis. Dual-anion dopants, such as N/S,^{187,198} P/S,¹⁹⁴ P/B,^{189,199} and N/P¹⁸⁸ have been employed to improve the performance of metal (hydr)oxides. Current studies suggest that dual-anion dopants can benefit the catalytic properties of metal (hydr)oxides via

different mechanisms. In a B/P co-doped NiVFe layered double hydroxide (LDH) catalyst, the B and P dopants can not only alter the electronic properties of NiVFe LDH but also generate rich defects and amorphous regions on the catalyst, thereby enhancing the intrinsic activities and populating active sites.¹⁸⁹ Differently, Kim et al. found that the N/S co-doping could boost the catalytic performance of amorphous Co-Ni-O nanocages by increasing the oxidation states of metals and accelerating the in situ generation of active CoOOH and NiOOH phases.¹⁹⁸ Lee and coauthors found that the P/B dual dopants would weaken the metal–metal bonds in amorphous Co-Mn-Ni-O, leading to efficient electron transfer.¹⁹⁹

TABLE 3 Representative anion–anion dual-doped metal catalysts for water electrolysis.

Catalyst	Synthetic method	Application	Electrolyte	Performance
N/S co-doped CoMoO ₄ ¹⁸⁷	Hydrothermal process, chemical vapor deposition	HER	1 M KOH	$\eta_{10} = 58$ mV, Tafel slope = 48.68 mV dec ⁻¹
N/P co-doped NiFe ₂ O ₄ ¹⁸⁸	Hydrothermal process, calcination, sonication	OER	1 M KOH	$\eta_{100} = 247$ mV, Tafel slope = 83.6 mV dec ⁻¹
B/P co-doped NiVFe-LDHs ¹⁸⁹	Hydrothermal process, boronization, and phosphorization	HER	1 M KOH	$\eta_{10} = 117$ mV, Tafel slope = 68 mV dec ⁻¹
S/Se co-doped NiFeOOH ¹⁹⁰	Oxidation	OER	1 M KOH	$\eta_{10} = 195$ mV, Tafel slope = 31.99 mV dec ⁻¹
N/P co-doped MoS ₂ ¹⁹¹	Sintering	HER	0.5 M H ₂ SO ₄	$\eta_{10} = 179$ mV, Tafel slope = 143 mV dec ⁻¹
O/P co-doped MoS ₂ ¹⁹²	Hydrothermal process	HER	0.5 M H ₂ SO ₄	$\eta_{50} = 227$ mV, Tafel slope = 54 mV dec ⁻¹
F/P co-doped NiSe ₂ ⁵¹	Hydrothermal process, fluorination, phosphorization, and selenization	HER	1 M KOH	$\eta_{10} = 53$ mV, Tafel slope = 95.6 mV dec ⁻¹
F/P co-doped NiCoN ¹⁹³	Solvothermal treatment and annealing	OER	1 M KOH	$\eta_{10} = 280$ mV, Tafel slope = 66.1 mV dec ⁻¹
S/P co-doped Co _x O _y /Cu@CuS ¹⁹⁴	Chemical-thermal reaction, electrodeposition, and phosphorization	HER	1 M KOH	$\eta_{10} = 116$ mV, Tafel slope = 59.2 mV dec ⁻¹
		OER	1 M KOH	$\eta_{10} = 280$ mV, Tafel slope = 73.9 mV dec ⁻¹
		OWS	1 M KOH	$E_{10} = 1.52$ V
N/F co-doped CoPO _x ¹⁹⁵	Ionothermal method and calcination	OER	1 M KOH	$\eta_{10} = 276$ mV, Tafel slope = 63.29 mV dec ⁻¹
N/S co-doped Mo ₂ C ¹⁹⁶	Hydrothermal process, calcination	HER	0.5 M H ₂ SO ₄	$\eta_{10} = 86$ mV, Tafel slope = 47 mV dec ⁻¹
Te/Cl co-doped NiFe MOFs ¹⁹⁷	Hydrothermal process, annealing	OER	1 M KOH	$\eta_{30} = 224$ mV, Tafel slope = 37.6 mV dec ⁻¹

Abbreviations: HER, hydrogen evolution reaction; MOFs, metal–organic framework; OER, oxygen evolution reaction; OWS, overall water electrolysis.

Developing oxide-based heterostructures (e.g., oxide/sulfide composites) is an effective route to boost the catalytic performance, which can take advantage of both oxides and sulfides.^{200,201} Anion dual doping can further regulate the catalytic properties of the oxide/sulfide composite. In the P/S co-doped Co_xO_y nanosheets grown on Cu@CuS nanowires (P,S-Co_xO_y/Cu@CuS NWs, Figure 8A), the doping of P and S in both Co₃O₄ and CoO leads to higher DOS values than that of single-doped oxides (Figure 8B–E). Thus, the P/S co-doping can enrich electron densities around the Fermi level and benefit the charge transfer performance for enhanced electrocatalytic properties. For OWS, the bifunctional P,S-Co_xO_y/Cu@CuS NWs show comparable performance to that of precious metal-based Pt/C||RuO₂/C electrodes (Figure 8F). In addition, The P,S-Co_xO_y/Cu@CuS NWs-driven water electrolysis system shows OER and HER Faradaic efficiencies of 99.65% and 99.76%, respectively

(Figure 8G), indicating the promising applications of cost-effective P,S-Co_xO_y/Cu@CuS NWs. Generally, the incorporation of S and P activates the activity of the cobalt oxide shell and thus leads to a high-performance oxide/sulfide composite. However, whether the anion doping process affects the electronic properties of the inner sulfide component and influences the oxide/sulfide electronic interaction remains unclear.

5.2 | Anion–anion dual-doped metal chalcogenides, pnictides, and others

For water electrolysis, dual anion-doped metal chalcogenides, pnictides, carbides, alloys, and MOFs gain growing interest for their high conductivity, rich active sites, and regulated electronic properties.²⁰² Anion dopants show different roles in enhancing these materials'

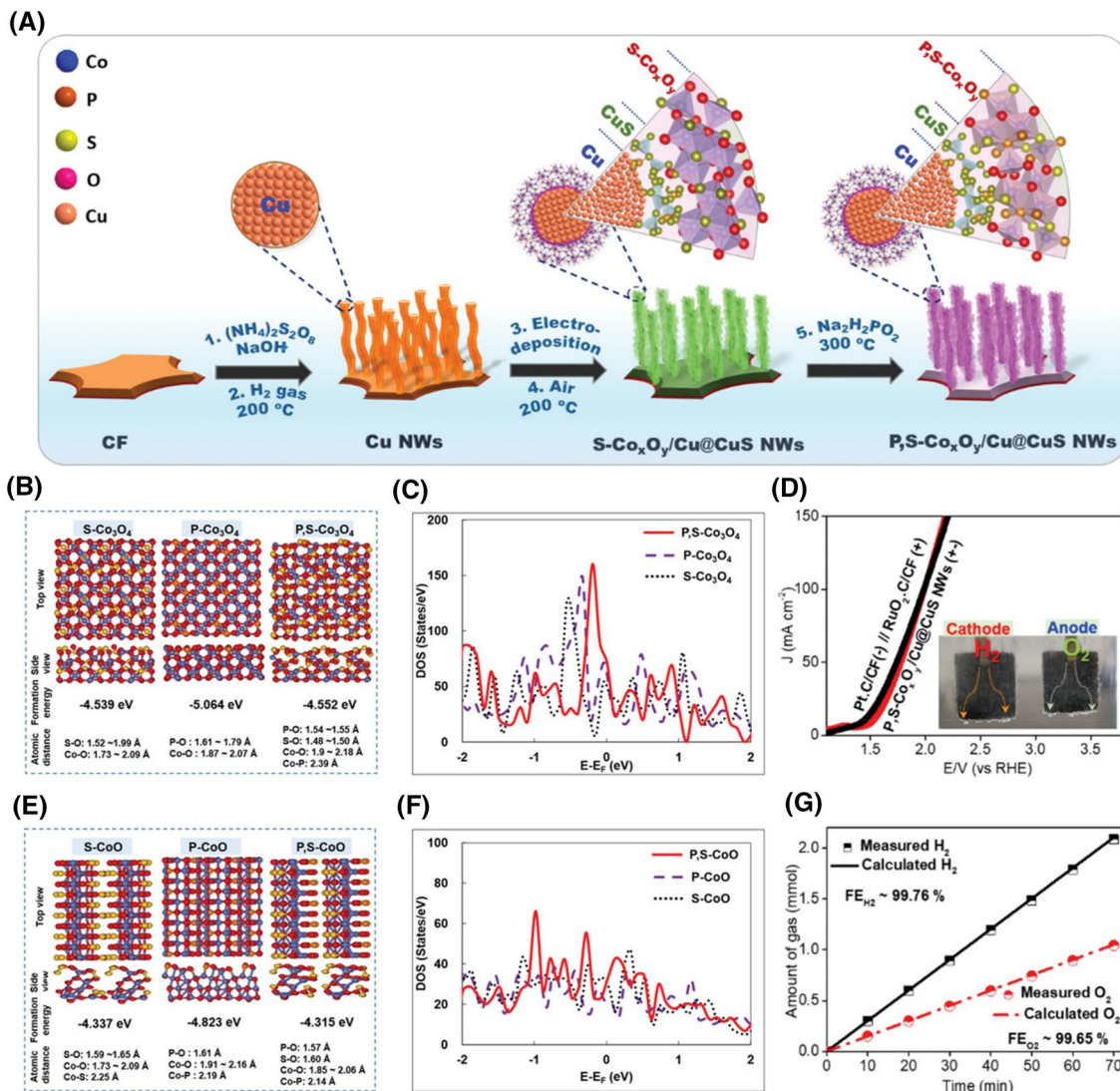


FIGURE 8 (A) Scheme of the synthesis of $\text{P,S-Co}_x\text{O}_y/\text{Cu}@/\text{CuS}$ NWs. (B) Optimized structures and (C) DOS of $\text{P-Co}_3\text{O}_4$, $\text{S-Co}_3\text{O}_4$, and $\text{P,S-Co}_3\text{O}_4$. (D) Optimized structures and (E) DOS of P-CoO , S-CoO , and $\text{P,S-Co}_3\text{O}_4$. (F) LSV curves for water splitting over bifunctional $\text{P,S-Co}_x\text{O}_y/\text{Cu}@/\text{CuS}$ NWs and $\text{Pt}/\text{C}||\text{RuO}_2/\text{C}$ electrode pairs. (G) Measured and calculated gas amounts of bifunctional $\text{P,S-Co}_x\text{O}_y/\text{Cu}@/\text{CuS}$ NWs during water electrolysis. Reproduced with permission.¹⁹⁴ Copyright 2020, Wiley. DOS, density of states; LSV, linear sweep voltammetry; NWs, nanowires catalysts.

catalytic performance, depending on the catalyst type and catalytic reaction. In a Se/S dual-doped Ni-Fe based catalyst, the presence of sacrificial Se and S accelerates the surface reconstruction of the catalyst during OER and promotes the evolution of the active NiFeOOH phase.¹⁹⁰ Working as an OER catalyst in alkalized seawater electrolyte, the self-formed $\text{NiFeOOH}(\text{S}, \text{Se})$ catalyst can achieve 100 mA cm^{-2} with a low overpotential of 0.239 V . Cl dopant in the Te/Cl co-doped NiFe MOF also shows an important role in boosting the structure reconstruction via etching during the OER process.¹⁹⁷ Moreover, in another F/P co-doped NiSe_2 HER catalyst synthesized with a three-step method (Figure 9A), the F and P dopants mainly help to regulate the electronic structure of

NiSe_2 .⁵¹ Figure 9B suggests that the F/P dual-doped catalyst ($\eta_{10} = 53\text{ mV}$) outperforms the single-doped and undoped analogs. Differential charge density analysis reveals the dopant-induced charge redistribution in the F/P co-doped NiSe_2 (Figure 9C,D). Compared with P, the F dopant gains more electrons from surrounding Ni sites due to the electronegativity of $\text{Ni} < \text{P} < \text{F}$ (Figure 9E-G). Thus, F dopant can regulate the potential side effects of P on the electronic properties of active Ni sites. The total DOS figures of F/P co-doped NiSe_2 and NiSe_2 indicate an improved intrinsic conductivity induced by F/P co-doping (Figure 9H). Further computational results imply that the ΔG_{H^*} of F/P co-doped NiSe_2 is closer to the thermal neutral than that of the

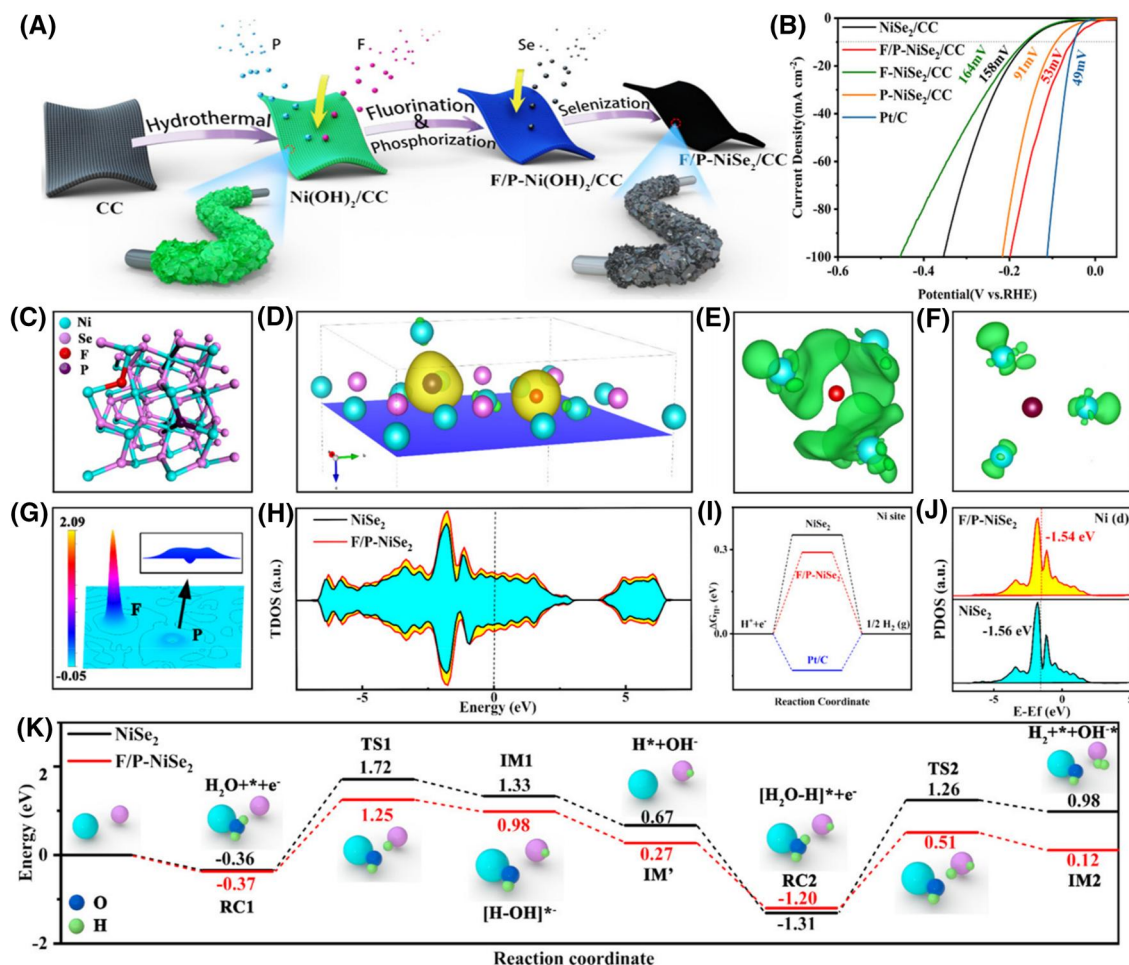


FIGURE 9 (A) Scheme of the fabrication of F/P-NiSe₂/CC. (B) HER LSV curves of Pt/C, F/P-NiSe₂/CC, P-NiSe₂/CC, F-NiSe₂/CC, and NiSe₂/CC. (C) Crystal structure of F/P-NiSe₂. (D) Charge density difference of F/P-NiSe₂. Electron loss in Ni around (E) F and (F) P. (G) Comparison of electrons gained by P and F. (H) Total DOS of F/P-NiSe₂ and NiSe₂. (I) ΔG_{H^*} of Pt/C, F/P-NiSe₂, and NiSe₂. (J) Project DOS of Ni d orbitals for F/P-NiSe₂ and NiSe₂. (K) Calculated HER free-energy profiles over F/P-NiSe₂ and NiSe₂. Reproduced with permission.⁵¹ Copyright 2022, American Chemical Society. DOS, density of states; HER, hydrogen evolution reaction; LSV, linear sweep voltammetry.

bare NiSe₂ (0.290 vs. 0.352 eV) (Figure 9I), which should be due to the elevated *d*-band center-induced enhanced intermediate adsorption over F/P-NiSe₂ (Figure 9J). In addition, the HER energy profiles suggest the reduced rate-limiting barrier with the F/P co-doped NiSe₂ catalyst (Figure 9K). By enhancing intrinsic conductivity and intrinsic activity, the F and P dual dopants help to elevate the HER performance of NiSe₂.

With a two-dimensional structure, MoS₂ and WS₂ are promising HER catalysts. To activate the inert basal plane of MoS₂/WS₂ and promote the 2H-to-1T phase transformation, dual anion doping has been developed. The introduction of N and P dopants in the basal plane of MoS₂ can trigger basal plane sites for water dissociation, hydride, and proton acceptance by forming novel Mo-N-P sites.²⁰³ However, Feng et al. found that the N and P dopants could realize the conversion of 2H MoS₂ to 1T MoS₂ and enlarge the interlayer spacing.¹⁹¹ Therefore,

the dual anion dopants help to improve the conductivity of MoS₂. In addition, DFT calculations found a smaller G_{H^*} value of 0.08 eV on N/P-MoS₂ than that of N-MoS₂ (0.73 eV), P-MoS₂ (0.67 eV), and MoS₂ (2.05 eV), suggesting enhanced HER intrinsic activity. In 2018, Maiti and coauthors found that N and P dual dopants could enhance the HER performance of WS₂.²⁰⁴ The N and P co-doping not only leads to the generation of a flake-like 1T phase structure with an expanded interlayer spacing than that in undoped WS₂ but also downshifts the *d*-band center and introduces rich S vacancies. As a result, the N/P co-doped WS₂ possesses high HER activities ($\eta_{10} = 59$ mV, Tafel slope = 35 mV dec⁻¹). O/P dual-doped MoS₂ also has high catalytic performance toward HER,¹⁹² while the mechanism for the dopant-induced electronic structure regulation is unclear.

To boost the performance of metal pnictides and carbides, dual-anion dopants such as N/S,^{196,205} N/F,¹⁹⁵

and P/F¹⁹³ have been developed. In these attempts, the role of anion dopants in electronic structure regulation is emphasized. For example, in the S/N co-doped MoP, electronegative dopants (N, S) can help stabilize P³⁻ via forming P–S and P–N bonds.²⁰⁵ Such electronic regulation further withdraws electrons from P and donates them back to the *d* orbital of Mo, thereby activating the Mo sites and promoting the HER performance. Besides the electronic property optimization, interestingly, Ang et al. found that the N/S dopants could significantly improve the wettability of Mo₂C and benefit the mass diffusion during the HER process.

6 | CONCLUSIONS AND PERSPECTIVES

Engineering efficient electrocatalysts for water splitting plays an important role in accelerating the commercialization of green hydrogen production. In this review, the advances in dual doping-mediated metal catalyst design have been comprehensively analyzed. Dual doping can enhance the catalytic performance of metal catalysts by regulating the electronic properties, improving the electrical conductivity, increasing the population of active sites, and improving stability. Depending on the species of dopants, cation–cation, cation–anion, and anion–anion dual doping techniques have been employed to upgrade the catalytic performance of metal (hydr)oxides, chalcogenides, pnictides, etc. Although great achievements have been made, some critical issues need further exploration.

- (1) Emphasize the importance of doping level. In this review, diverse dual dopants have been analyzed to enhance the performance of metal electrocatalysts. In most cases, researchers mainly focus on dopant species, while the effect of doping levels on the catalytic activity has not been well illustrated. As suggested by previous studies, doping levels can significantly influence the performance of catalysts by regulating their electronic properties.^{127,206} In this context, it is necessary to optimize the doping level of dual dopants for achieving high-performance catalysts. In addition, some sacrificial dopants (e.g., Al, Zn, B, S, and Cl) will be etched during electrocatalysis and release more electroactive sites and defects,^{114,143} but a high level of such sacrificial dopants may lead to diminished stability. Thus, controlling the doping level of sacrificial dopants can help to balance the activity and stability of catalysts.
- (2) Figure out real active sites of dual-doped electrocatalysts. Most metal catalysts are suggested to undergo structure transformation during the OER or

HER process. How do dual dopants affect the structure evolution process? Whether dopants will be leached out during the catalytic process? Do dual dopants act as active sites or just help to regulate the electronic properties of self-evolved structures? These questions are important for understanding the behavior and effect of dual dopants and the real active sites of metal catalysts during working conditions. Therefore, more attention should be paid to understanding the dynamic structure evolution of dual-doped electrocatalysts with *in situ* techniques. In addition, HRTEM images of catalysts before and after catalysis are beneficial for checking the potential structure transformation, element dissolution, defect formation, and surface amorphization of dual-doped catalysts.

- (3) Accelerate the catalyst design via machine learning. As shown in Tables 1–3, different elements can be used as dual dopants to enhance the performance of metal catalysts. However, the rational design of dual-doped catalysts remains based on trial-and-error methods, which takes a long time and complicated synthetic processes. To accelerate the design of dual-doped metal catalysts, machine learning is a promising tool to find suitable dopants with geometrical, electronic, and activity descriptors obtained from DFT calculations. By calculating the interaction between dual-doped electrocatalysts and reaction intermediates (e.g., *OH, *H, and *OOH), it is feasible to obtain catalysts with favorable dopants. Furthermore, computational results related to catalysts' electronic properties (e.g., work function, *d*-band center, *p*-band center, charge density, orbital filling, and orbital orientation) can be used to screen promising dopants. A critical precondition of DFT calculations is the determination of precise crystal structures of dual-doped catalysts, especially the position and concentration of dual dopants.

ACKNOWLEDGMENTS

This work is supported by the Australian Research Council (ARC) Discovery Project (DP220101139).

CONFLICT OF INTEREST STATEMENT

There is no conflict of interest.

DATA AVAILABILITY STATEMENT

Data sharing is not applicable to this article as no datasets were generated or analyzed during the current study.

ORCID

Zhijie Chen  <https://orcid.org/0000-0003-0627-0856>

REFERENCES

- Zheng X, Xue Y, Chen S, Li Y. Advances in hydrogen energy conversion of graphdiyne-based materials. *EcoEnergy*. 2023; 1(1):45-59.
- Chen Z, Duan X, Wei W, Wang S, Ni B-J. Recent advances in transition metal-based electrocatalysts for alkaline hydrogen evolution. *J Mater Chem A*. 2019;7(25):14971-15005.
- Terlouw T, Bauer C, McKenna R, Mazzotti M. Large-scale hydrogen production via water electrolysis: a techno-economic and environmental assessment. *Energy Environ Sci*. 2022;15(9):3583-3602.
- Fu G, Kang X, Zhang Y, et al. Coordination effect-promoted durable Ni(OH)₂ for energy-saving hydrogen evolution from water/methanol co-electrocatalysis. *Nano-Micro Lett*. 2022; 14(1):200.
- Chen Z, Wei W, Song L, Ni B-J. Hybrid water electrolysis: a new sustainable avenue for energy-saving hydrogen production. *Sustain Horiz*. 2022;1:100002.
- Deng C, Toe CY, Li X, et al. Earth-abundant metal-based electrocatalysts promoted anodic reaction in hybrid water electrolysis for efficient hydrogen production: recent progress and perspectives. *Adv Energy Mater*. 2022;12(25):2201047.
- Wang T, Tao L, Zhu X, et al. Combined anodic and cathodic hydrogen production from aldehyde oxidation and hydrogen evolution reaction. *Nat Catal*. 2022;5(1):66-73.
- Chen Z, Duan X, Wei W, Wang S, Ni B-J. Electrocatalysts for acidic oxygen evolution reaction: achievements and perspectives. *Nano Energy*. 2020;78:105392.
- You N, Cao S, Huang M, et al. Constructing P-CoMoO₄@NiCoP heterostructure nanoarrays on Ni foam as efficient bifunctional electrocatalysts for overall water splitting. *Nano Mater Sci*. 2023;5(3):278-286.
- Zhang Y, Zheng W, Wu H, et al. Tungsten oxide-anchored Ru clusters with electron-rich and anti-corrosive microenvironments for efficient and robust seawater splitting. *SusMat*. 2024;4:106-115.
- Guo B, Ding Y, Huo H, et al. Recent advances of transition metal basic salts for electrocatalytic oxygen evolution reaction and overall water electrolysis. *Nano-Micro Lett*. 2023;15(1):57.
- Chen Z, Wei W, Ni B-J. Cost-effective catalysts for renewable hydrogen production via electrochemical water splitting: recent advances. *Curr Opin Green Sustainable Chem*. 2021; 27:100398.
- Hou L, Jang H, Gu X, et al. Design strategies of ruthenium-based materials toward alkaline hydrogen evolution reaction. *EcoEnergy*. 2023;1(1):16-44.
- Wang J, Gao Y, Kong H, et al. Non-precious-metal catalysts for alkaline water electrolysis: operando characterizations, theoretical calculations, and recent advances. *Chem Soc Rev*. 2020;49(24):9154-9196.
- Anantharaj S, Noda S, Jothi VR, Yi S, Driess M, Menezes PW. Strategies and perspectives to catch the missing pieces in energy-efficient hydrogen evolution reaction in alkaline media. *Angew Chem Int Ed*. 2021;60(35):18981-19006.
- Chen Z, Duan X, Wei W, Wang S, Ni B-J. Iridium-based nanomaterials for electrochemical water splitting. *Nano Energy*. 2020;78:105270.
- Li X, Xu W, Fang Y, et al. Single-atom catalyst application in distributed renewable energy conversion and storage. *Sus-Mat*. 2023;3(2):160-179.
- Xu K, Sun Y, Sun Y, et al. Yin-Yang harmony: metal and nonmetal dual-doping boosts electrocatalytic activity for alkaline hydrogen evolution. *ACS Energy Lett*. 2018;3(11): 2750-2756.
- Sun J-P, Zheng Y, Zhang Z-S, Meng X-C, Li Z-Z. Modulation of *d*-orbital to realize enriched electronic cobalt sites in cobalt sulfide for enhanced hydrogen evolution in electrocatalytic water/seawater splitting. *Rare Met*. 2023; 43(2):511-521.
- Zhou YN, Yu WL, Liu HJ, et al. Self-integration exactly constructing oxygen-modified MoNi alloys for efficient hydrogen evolution. *EcoEnergy*. 2023;1(2):425-436.
- Chen Z, Yun S, Wu L, et al. Waste-derived catalysts for water electrolysis: circular economy-driven sustainable green hydrogen energy. *Nano-Micro Lett*. 2023;15(1):4.
- Ma M-Y, Yu H-Z, Deng L-M, et al. Interfacial engineering of heterostructured carbon-supported molybdenum cobalt sulfides for efficient overall water splitting. *Tungsten*. 2023;5(4): 589-597.
- Zhu Y, Liu X, Jin S, et al. Anionic defect engineering of transition metal oxides for oxygen reduction and evolution reactions. *J Mater Chem A*. 2019;7(11):5875-5897.
- Li S, Liu D, Wang G, et al. Vertical 3D nanostructures boost efficient hydrogen production coupled with glycerol oxidation under alkaline conditions. *Nano-Micro Lett*. 2023; 15(1):189.
- Liu D, Ai H, Li J, et al. Surface reconstruction and phase transition on vanadium-cobalt-iron trimetal nitrides to form active oxyhydroxide for enhanced electrocatalytic water oxidation. *Adv Energy Mater*. 2020;10(45).
- Ede SR, Luo Z. Tuning the intrinsic catalytic activities of oxygen-evolution catalysts by doping: a comprehensive review. *J Mater Chem A*. 2021;9(36):20131-20163.
- Zhang J, Zhang J, He F, et al. Defect and doping co-engineered non-metal nanocarbon ORR electrocatalyst. *Nano-Micro Lett*. 2021;13:1-30.
- Fan M, Yuan Q, Zhao Y, et al. A facile "double-catalysts" approach to directionally fabricate pyridinic N-B-pair-doped crystal graphene nanoribbons/amorphous carbon hybrid electrocatalysts for efficient oxygen reduction reaction. *Adv Mater*. 2022;34(13):2107040.
- Hao S, Wang Y, Zheng G, et al. Tuning electronic correlations of ultra-small IrO₂ nanoparticles with La and Pt for enhanced oxygen evolution performance and long-durable stability in acidic media. *Appl Catal B Environ*. 2020;266:118643.
- Li P, Bi J, Liu J, et al. In situ dual doping for constructing efficient CO₂-to-methanol electrocatalysts. *Nat Commun*. 2022;13(1):1965.
- Guo L, Chi J, Zhu J, Cui T, Lai J, Wang L. Dual-doping NiMoO₄ with multi-channel structure enable urea-assisted energy-saving H₂ production at large current density in alkaline seawater. *Appl Catal B Environ*. 2023;320:121977.
- Chang J, Wang G, Yang Z, et al. Dual-doping and synergism toward high-performance seawater electrolysis. *Adv Mater*. 2021;33(33):2101425.

33. Zhai X, Yu Q, Chi J, et al. Accelerated dehydrogenation kinetics through Ru, Fe dual-doped Ni₂P as bifunctional electrocatalyst for hydrazine-assisted self-powered hydrogen generation. *Nano Energy*. 2023;105:108008.
34. Chatenet M, Pollet BG, Dekel DR, et al. Water electrolysis: from textbook knowledge to the latest scientific strategies and industrial developments. *Chem Soc Rev*. 2022;51(11):4583-4762.
35. Yang H, Driess M, Menezes PW. Self-supported electrocatalysts for practical water electrolysis. *Adv Energy Mater*. 2021;11(39):2102074.
36. Liu R-T, Xu Z-L, Li F-M, et al. Recent advances in proton exchange membrane water electrolysis. *Chem Soc Rev*. 2023;52(16):5652-5683.
37. Al-Naggar AH, Shinde NM, Kim J-S, Mane RS. Water splitting performance of metal and non-metal-doped transition metal oxide electrocatalysts. *Coord Chem Rev*. 2023;474:214864.
38. Xu X, Su C, Zhou W, Zhu Y, Chen Y, Shao Z. Co-doping strategy for developing perovskite oxides as highly efficient electrocatalysts for oxygen evolution reaction. *Adv Sci*. 2016;3(2):1500187.
39. Sun J, Du L, Sun B, et al. A bifunctional perovskite oxide catalyst: the triggered oxygen reduction/evolution electrocatalysis by moderated Mn-Ni co-doping. *J Energy Chem*. 2021;54:217-224.
40. Dong J, Lu Y, Tian X, et al. Genuine active species generated from Fe₃N nanotube by synergistic CoNi doping for boosted oxygen evolution catalysis. *Small*. 2020;16(40):2003824.
41. Hu Y, Huang D, Zhang J, Huang Y, Balogun M-SJT, Tong Y. Dual doping induced interfacial engineering of Fe₂N/Fe₃N hybrids with favorable *d*-band towards efficient overall water splitting. *ChemCatChem*. 2019;11(24):6051-6060.
42. Yang C, Wang C, Zhou L, et al. Refining *d*-band center in NiO. 85Se by Mo doping: a strategy for boosting hydrogen generation via coupling electrocatalytic oxidation 5-hydroxymethylfurfural. *Chem Eng J*. 2021;422:130125.
43. Liao Y, He R, Pan W, et al. Lattice distortion induced Ce-doped NiFe-LDH for efficient oxygen evolution. *Chem Eng J*. 2023;464:142669.
44. Du Q, Su P, Cao Z, Yang J, Price CAH, Liu J. Construction of N and Fe co-doped CoO/CoxN interface for excellent OER performance. *Sustain Mater Technol*. 2021;29:e00293.
45. Wang P, Zhang L, Wang Z, et al. N and Mn dual-doped cactus-like cobalt oxide nanoarchitecture derived from cobalt carbonate hydroxide as efficient electrocatalysts for oxygen evolution reactions. *J Colloid Interface Sci*. 2021;597:361-369.
46. Wang J, Liao T, Wei Z, Sun J, Guo J, Sun Z. Heteroatom-doping of non-noble metal-based catalysts for electrocatalytic hydrogen evolution: an electronic structure tuning strategy. *Small Methods*. 2021;5(4):2000988.
47. Bolar S, Shit S, Murmu NC, Samanta P, Kuila T. Activation strategy of MoS₂ as HER electrocatalyst through doping-induced lattice strain, band gap engineering, and active crystal plane design. *ACS Appl Mater Interfaces*. 2021;13(1):765-780.
48. Munawar T, Mukhtar F, Nadeem MS, et al. Facile synthesis of rare earth metal dual-doped Pr₂O₃ nanostructures: enhanced electrochemical water-splitting and antimicrobial properties. *Ceram Int*. 2022;48(13):19150-19165.
49. Singh VK, Nakate UT, Bhuyan P, Chen J, Tran DT, Park S. Mo/Co doped 1T-VS₂ nanostructures as a superior bifunctional electrocatalyst for overall water splitting in alkaline media. *J Mater Chem A*. 2022;10(16):9067-9079.
50. Gao B, Du X, Zhao Y, et al. Electron strain-driven phase transformation in transition-metal-co doped MoTe₂ for electrocatalytic hydrogen evolution. *Chem Eng J*. 2022;433:133768.
51. Yuan W, Li Y, Liang L, Wang F, Liu H. Dual-anion doping enables NiSe₂ electrocatalysts to accelerate alkaline hydrogen evolution reaction. *ACS Appl Energy Mater*. 2022;5(4):5036-5043.
52. Xiao W, Zhang L, Bukhvalov D, et al. Hierarchical ultrathin carbon encapsulating transition metal doped MoP electrocatalysts for efficient and pH-universal hydrogen evolution reaction. *Nano Energy*. 2020;70:104445.
53. Qi J, Wang H, Lin J, et al. Mn and S dual-doping of MOF-derived Co₃O₄ electrode array increases the efficiency of electrocatalytic generation of oxygen. *J Colloid Interface Sci*. 2019;557:28-33.
54. Li M-X, Xiao B, Zhao Z-Y, et al. Morphology evolution regulation of dual-doped S, Fe-NiMoO₄ microrods based on precipitation-dissolution equilibrium for oxygen evolution. *Fuel*. 2023;336:126769.
55. Ali U, Sohail K, Liu Y, Yu X, Xing S. Molybdenum and phosphorous dual-doped, transition-metal-based, free-standing electrode for overall water splitting. *Chemelectrochem*. 2021;8(9):1612-1620.
56. Sahoo MK, Lee HH, Yang WS, Kim DS, Cho HK. Synergistic Mo and S co-doping on NiSe₂ electrodes for reduced kinetic barrier of water electrolysis. *Int J Hydrogen Energy*. 2023;49:25-36.
57. Mu J, Xu J, Zhou C, et al. Self-supported oxygen and molybdenum dual-doped cobalt phosphide hierarchical nanomaterials as superior bifunctional electrocatalysts for overall water splitting. *Chemelectrochem*. 2021;8(1):103-111.
58. Li K, Ding H, Zhou J-J, et al. Nitrogen and molybdenum co-doped CoP nanohoneycombs on 3D nitrogen-doped porous graphene as enhanced electrocatalyst for oxygen evolution reaction. *Int J Hydrogen Energy*. 2021;46(72):35585-35593.
59. Zhang Z, Song N, Wang J, Liu Y, Dai Z, Nie G. Polydopamine-derived carbon layer anchoring NiCo-P nanowire arrays for high-performance binder-free supercapacitor and electrocatalytic hydrogen evolution. *SusMat*. 2022;2(5):646-657.
60. Wang J-H, Yang S-W, Ma F-B, et al. RuCo alloy nanoparticles embedded within N-doped porous two-dimensional carbon nanosheets: a high-performance hydrogen evolution reaction catalyst. *Tungsten*. 2023;6(1):114-123.
61. Liu W, Que W, Yin R, et al. Ferrum-molybdenum dual incorporated cobalt oxides as efficient bifunctional anti-corrosion electrocatalyst for seawater splitting. *Appl Catal B Environ*. 2023;328:122488.
62. He J, Li W, Xu P, Sun J. Tuning electron correlations of RuO₂ by co-doping of Mo and Ce for boosting electrocatalytic water oxidation in acidic media. *Appl Catal B Environ*. 2021;298:120528.

63. He J, Fu G, Zhang J, Xu P, Sun J. Multistage electron distribution engineering of iridium oxide by codoping W and Sn for enhanced acidic water oxidation electrocatalysis. *Small*. 2022;18(41):2203365.
64. Hao S, Liu M, Pan J, et al. Dopants fixation of Ruthenium for boosting acidic oxygen evolution stability and activity. *Nat Commun*. 2020;11(1):5368.
65. Guo B, Ma R, Li Z, Luo J, Yang M, Wang J. Dual-doping of ruthenium and nickel into Co_3O_4 for improving the oxygen evolution activity. *Mater Chem Front*. 2020;4(5):1390-1396.
66. Cui T, Zhai X, Guo L, et al. Controllable synthesis of a self-assembled ultralow Ru, Ni-doped Fe_2O_3 lily as a bifunctional electrocatalyst for large-current-density alkaline seawater electrolysis. *Chin J Catal*. 2022;43(8):2202-2211.
67. He H, Chen H, Chen J, et al. Dual sites modulating MoO_2 nanospheres for synergistically enhanced electrocatalysis of water oxidation. *Chem Eng J*. 2022;443:136339.
68. Xu H, Wang C, Huang B, Shang H, Du Y. Dual-cation doping precisely reducing the energy barrier of the rate-determining step for promoting oxygen-evolving activity. *Inorg Chem Front*. 2023;10(7):2067-2074.
69. Qin J-F, Yang M, Hou S, et al. Copper and cobalt co-doped Ni_3S_2 grown on nickel foam for highly efficient oxygen evolution reaction. *Appl Surf Sci*. 2020;502:144172.
70. Duan J-J, Han Z, Zhang R-L, et al. Iron, manganese co-doped Ni_3S_2 nanoflowers in situ assembled by ultrathin nanosheets as a robust electrocatalyst for oxygen evolution reaction. *J Colloid Interface Sci*. 2021;588:248-256.
71. Han D, Luo Z, Li Y, et al. Synergistic engineering of MoS_2 via dual-metal doping strategy towards hydrogen evolution reaction. *Appl Surf Sci*. 2020;529:147117.
72. Guo F-b, Zhao X-y, Lei H-y, et al. Bimetallic doping-derived heterostructures in NiCo-WSe_2 to promote hydrogen evolution reaction. *J Alloys Compd*. 2022;924:166538.
73. Li X, Huang J, Feng L, et al. Molybdenum and cobalt co-doped VC nanoparticles encapsulated in nanocarbon as efficient electrocatalysts for the hydrogen evolution reaction. *Inorg Chem Front*. 2022;9(5):870-878.
74. Ma G, Qin M, Fan Z, Chen Y, Xin X. Manganese, iron co-doped Ni_2P nanoflowers as a powerful electrocatalyst for oxygen evolution reaction. *J Electroanal Chem*. 2022;921:116681.
75. Song Y, Cheng J, Liu J, et al. Modulating electronic structure of cobalt phosphide porous nanofiber by ruthenium and nickel dual doping for highly-efficiency overall water splitting at high current density. *Appl Catal B Environ*. 2021;298:120488.
76. Chen Z, Wei W, Zou W, et al. Integrating electrodeposition with electrolysis for closing loop resource utilization of battery industrial wastewater. *Green Chem*. 2022;44:3208-3217.
77. Li X-X, Liu X-C, Liu C, Zeng J-M, Qi X-P. Co_3O_4 /stainless steel catalyst with synergistic effect of oxygen vacancies and phosphorus doping for overall water splitting. *Tungsten*. 2023;5(1):100-108.
78. Qian J, Zhang Y, Chen Z, Du Y, Ni B-J. NiCo layered double hydroxides/NiFe layered double hydroxides composite (NiCo-LDH/NiFe-LDH) towards efficient oxygen evolution in different water matrices. *Chemosphere*. 2023;345:140472.
79. Lee YJ, Park S-K. Synergistically coupling of Ni-Fe LDH arrays with hollow Co-Mo sulfide nanotriangles for highly efficient overall water splitting. *Rare Met*. 2023;43(2):522-532.
80. Chen Z, Wei W, Shon HK, Ni B-J. Designing bifunctional catalysts for urea electrolysis: progress and perspectives. *Green Chem*. 2024;26(2):631-654.
81. Amer MS, Arunachalam P, Ghanem MA, et al. Synthesis of iron and vanadium co-doped mesoporous cobalt oxide: an efficient and robust catalysts for electrochemical water oxidation. *Int J Energy Res*. 2021;45(6):9422-9437.
82. Hu W, Tian M, Zeng K, et al. Tuning the electronic structure of $\text{W}_{18}\text{O}_{49}$ via dual doping for efficient oxygen evolution reaction. *ACS Appl Energy Mater*. 2022;5(3):3208-3216.
83. Selvakumar K, Duraisamy V, Venkateshwaran S, et al. Development of $\alpha\text{-MnO}_2$ nanowire with Ni- and (Ni, Co)-cation doping as an efficient bifunctional oxygen evolution and oxygen reduction reaction catalyst. *Chemelectrochem*. 2022;9(2):e202101303.
84. Hilal ME, Şanlı SB, Dekyvere S, et al. A dual-doping strategy of LaCoO_3 for optimized oxygen evolution reaction toward zinc-air batteries application. *Int J Energy Res*. 2022;46(15):22014-22024.
85. Guo Q, Li X, Wei H, et al. Fe Co-doped perovskite oxides with high performance for oxygen evolution reaction. *Front Chem*. 2019;7:224.
86. Tang L, Fan T, Chen Z, et al. Binary-dopant promoted lattice oxygen participation in OER on cobaltate electrocatalyst. *Chem Eng J*. 2021;417:129324.
87. Guo F, Chen Q, Liu Z, Cheng D, Han N, Chen Z. Repurposing mining and metallurgical waste as electroactive materials for advanced energy applications: advances and perspectives. *Catalysts*. 2023;13(9):1241.
88. Li Y, Du X, Huang J, et al. Recent progress on surface reconstruction of earth-abundant electrocatalysts for water oxidation. *Small*. 2019;15(35):e1901980.
89. Pan J, Hao S, Zhang X, Huang R. In situ growth of Fe and Nb co-doped $\beta\text{-Ni(OH)}_2$ nanosheet arrays on nickel foam for an efficient oxygen evolution reaction. *Inorg Chem Front*. 2020;7(18):3465-3474.
90. Li R, Ren P, Yang P, et al. Bimetallic co-doping engineering over nickel-based oxy-hydroxide enables high-performance electrocatalytic oxygen evolution. *J Colloid Interface Sci*. 2023;631:173-181.
91. Wei Y, Yi L, Wang R, et al. A unique etching-doping route to Fe/Mo Co-doped Ni oxyhydroxide catalyst for enhanced oxygen evolution reaction. *Small*. 2023;19(37):2301267.
92. Jiang J, Sun F, Zhou S, et al. Atomic-level insight into super-efficient electrocatalytic oxygen evolution on iron and vanadium co-doped nickel (oxy)hydroxide. *Nat Commun*. 2018;9(1):2885.
93. Chen Z, Ibrahim I, Hao D, et al. Controllable design of nanoworm-like nickel sulfides for efficient electrochemical water splitting in alkaline media. *Mater Today Energy*. 2020;18:100573.
94. Yang J, Zheng M, Wu Y, et al. Unraveling the dominance of intrinsic catalytic activities over electrical properties in electrocatalytic performance of two-dimensional chromium

- chalcogenide nanosheets. *Appl Catal B Environ.* 2024;343:123478.
95. Nath M, Singh H, Saxena A. Progress of transition metal chalcogenides as efficient electrocatalysts for energy conversion. *Curr Opin Electrochem.* 2022;34:100993.
 96. Chen Z, Zheng R, Wei W, Ni B-J, Chen H. Unlocking the electrocatalytic activity of natural chalcopyrite using mechanochemistry. *J Energy Chem.* 2022;68:275-283.
 97. Du X, Li J, Zhang X. Fe and Cu dual-doped Ni₃S₄ nanoarrays with less low-valence Ni species for boosting water oxidation reaction. *Dalton Trans.* 2022;51(4):1594-1602.
 98. Bai L, Cao W, Du X, Wang Y, Wu L, Li J. Cobalt and vanadium dual-doping engineering of NiS/Ni₇S₆ with heterogeneous interface as efficient electrocatalyst for the oxygen evolution reaction. *J Alloys Compd.* 2023;960:170652.
 99. Liu L, Zhang Y, Wang J, et al. In situ growth Fe and V co-doped Ni₃S₂ for efficient oxygen evolution reaction at large current densities. *Int J Hydrogen Energy.* 2022;47(32):14422-14431.
 100. Ai T, Wang H, Bao W, et al. Fe-V synergistic doping effect of hierarchical Ni₃S₂ oblate-nanorod arrays for efficient electrocatalytic oxygen evolution reaction. *Chem Eng J.* 2022; 450:138358.
 101. Mao X, Liu Y, Chen Z, Fan Y, Shen P. Fe and Co dual-doped Ni₃S₄ nanosheet with enriched high-valence Ni sites for efficient oxygen evolution reaction. *Chem Eng J.* 2022; 427:130742.
 102. Li J, Zhang L, Du X, Zhang X. Co, Mn co-doped Fe₉S₁₁@Ni₉S₈ supported on nickel foam as a high efficiency electrocatalyst for the oxygen evolution reaction and urea oxidation reaction. *Dalton Trans.* 2022;51(26):10249-10256.
 103. Zhou C, Wu H, Zhang F, Miao Y. Cobalt, ferrum co-doped Ni₃Se₄ nano-flake array: an efficient electrocatalyst for the alkaline hydrogen evolution and overall water splitting. *Crystals.* 2022;12(5):666.
 104. Tuo Y, Wang X, Chen C, et al. Identifying the role of Ni and Fe in Ni-Fe co-doped orthorhombic CoSe₂ for driving enhanced electrocatalytic activity for oxygen evolution reaction. *Electrochim Acta.* 2020;335:135682.
 105. Wu C, Du Y, Fu Y, et al. Co co-doped NiS bulks supported on Ni foam as an efficient electrocatalyst for overall water splitting in alkaline media. *Sustain Energy Fuels.* 2020; 4(4):1654-1664.
 106. Krishnamurthy P, Kumar A, Alqarni SA, Silambarasan S, Maiyalagan T. Iron and vanadium co-doped Ni₃S₂ flower like nanosheets as an efficient electrocatalysts for water splitting. *Surf Interfaces.* 2024;44:103694.
 107. Chen L, Jang H, Kim MG, Qin Q, Liu X, Cho J. Fe, Al-co-doped NiSe₂ nanoparticles on reduced graphene oxide as an efficient bifunctional electrocatalyst for overall water splitting. *Nanoscale.* 2020;12(25):13680-13687.
 108. Gao C, Rao D, Yang H, et al. Dual transition-metal atoms doping: an effective route to promote the ORR and OER activity on MoTe₂. *New J Chem.* 2021;45(12):5589-5595.
 109. Nguyen DC, Luyen Doan TL, Prabhakaran S, et al. Hierarchical Co and Nb dual-doped MoS₂ nanosheets shelled micro-TiO₂ hollow spheres as effective multifunctional electrocatalysts for HER, OER, and ORR. *Nano Energy.* 2021;82:105750.
 110. Chen Z, Wei W, Ni B-J. Transition metal chalcogenides as emerging electrocatalysts for urea electrolysis. *Curr Opin Electrochem.* 2021;31:100888.
 111. Chen Z, Han N, Zheng R, Ren Z, Wei W, Ni BJ. Design of earth-abundant amorphous transition metal-based catalysts for electrooxidation of small molecules: advances and perspectives. *SusMat.* 2023;3(3):290-319.
 112. Zhao Y, Zhao X, Zhou Y, et al. Bimetallic co-doped CoP nanoflower arrays for efficient and stable overall water splitting. *Int J Hydrogen Energy.* 2023;51:276-284.
 113. Liu Y, Zhang Z, Zhang L, et al. Manipulating the d-band centers of transition metal phosphides through dual metal doping towards robust overall water splitting. *J Mater Chem A.* 2022;10(41):22125-22134.
 114. Wang P, Liu X, Yan Y, Cao J, Feng J, Qi J. Exploring CoP core-shell nanosheets by Fe and Zn dual cation doping as efficient electrocatalysts for overall water splitting. *Catal Sci Technol.* 2020;10(5):1395-1400.
 115. Lei S, Li Q, Luo Y, et al. Efficient electrocatalyst for solar-driven electrolytic water splitting: phosphorus (P) and niobium (Nb) co-doped NiFe₂O₄ nanosheet. *J Colloid Interface Sci.* 2023;651:818-828.
 116. Yang L, Yu J, Wei Z, et al. Co-N-doped MoO₂ nanowires as efficient electrocatalysts for the oxygen reduction reaction and hydrogen evolution reaction. *Nano Energy.* 2017; 41:772-779.
 117. Xie M, Jia K, Lu J, Zhao R. Bi-functional Mo and P co-doped ZnCo-LDH nanosheets as high performance electrocatalysts for boosting overall water splitting. *CrystEngComm.* 2020; 22(3):546-553.
 118. Song H, Wang J, Zhang Z, Shai X, Guo Y. Synergistic balancing hydrogen and hydroxyl adsorption/desorption of nickel sulfide via cation and anion dual-doping for boosting alkaline hydrogen evolution. *Chem Eng J.* 2021;420: 129842.
 119. Xing Y, Li D, Li L, Tong H, Jiang D, Shi W. Accelerating water dissociation kinetic in Co₉S₈ electrocatalyst by mn/N Co-doping toward efficient alkaline hydrogen evolution. *Int J Hydrogen Energy.* 2021;46(11):7989-8001.
 120. Zhang Y, Yang T, Li J, Zhang Q, Li B, Gao M. Construction of Ru, O Co-doping MoS₂ for hydrogen evolution reaction electrocatalyst and surface-enhanced Raman scattering substrate: high-performance, recyclable, and durability improvement. *Adv Funct Mater.* 2023;33(3):2210939.
 121. Yang H, Hu Y, Huang D, et al. Efficient hydrogen and oxygen evolution electrocatalysis by cobalt and phosphorus dual-doped vanadium nitride nanowires. *Mater Today Chem.* 2019;11:1-7.
 122. Xu B, Yang X, Fang Q, et al. Anion-cation dual doping: an effective electronic modulation strategy of Ni₂P for high-performance oxygen evolution. *J Energy Chem.* 2020;48: 116-121.
 123. Zhu J, Zheng X, Liu C, et al. Zinc and fluorine ions dual-modulated NiCoP nanoprism array electrocatalysts for efficient water splitting. *J Colloid Interface Sci.* 2023;630:559-569.
 124. Wang X, Hu Q, Li G, Wei S, Yang H, He C. Regulation of the adsorption sites of Ni₂P by Ru and S co-doping for ultra-efficient alkaline hydrogen evolution. *J Mater Chem A.* 2021;9(28):15648-15653.

125. Zhou Y, Xu J, Lian C, et al. Carbon impurity-free, novel Mn, N co-doped porous Mo₂C nanorods for an efficient and stable hydrogen evolution reaction. *Inorg Chem Front.* 2019;6(9):2464-2471.
126. Li Z, Xu S, Chu K, et al. Synergistic tuning of the electronic structure of Mo₂C by P and Ni codoping for optimizing electrocatalytic hydrogen evolution. *Inorg Chem.* 2020;59(18):13741-13748.
127. Chen Z, Zheng R, Graš M, et al. Tuning electronic property and surface reconstruction of amorphous iron borides via W-P co-doping for highly efficient oxygen evolution. *Appl Catal B Environ.* 2021;288:120037.
128. Mao Q, Jiao S, Ren K, et al. Transition metal and phosphorus co-doping induced lattice strain in mesoporous Rh-based nanospheres for pH-universal hydrogen evolution electrocatalysis. *Chem Eng J.* 2021;426:131227.
129. Liu Y, Ye C, Zhao S-N, et al. A dual-site doping strategy for developing efficient perovskite oxide electrocatalysts towards oxygen evolution reaction. *Nano Energy.* 2022;99:107344.
130. Ye Q, Liu J, Lin L, Sun M, Wang Y, Cheng Y. Fe and P dual-doped nickel carbonate hydroxide/carbon nanotube hybrid electrocatalysts for an efficient oxygen evolution reaction. *Nanoscale.* 2022;14(17):6648-6655.
131. Li T-F, Li J, Zhang L-P, et al. Work-function-induced interfacial electron redistribution of MoO₂/WO₂ heterostructures for high-efficiency electrocatalytic hydrogen evolution reaction. *Rare Met.* 2023;43(2):489-499.
132. Hao Y, Du G, Fan Y, et al. Mo/P dual-doped Co/oxygen-deficient Co₃O₄ core-shell nanorods supported on Ni foam for electrochemical overall water splitting. *ACS Appl Mater Interfaces.* 2021;13(46):55263-55271.
133. Li Z, Xue K-H, Wang J, et al. Cation and anion co-doped perovskite nanofibers for highly efficient electrocatalytic oxygen evolution. *ACS Appl Mater Interfaces.* 2020;12(37):41259-41268.
134. Zhang D, Wang Y, Du X, Zhang X. Iron and phosphorus dual-doped NiMoO₄ with nanorod structure as efficient oxygen evolution catalyst in alkaline seawater. *Int J Hydrogen Energy.* 2024;49:1387-1398.
135. Lyu C, Li Y, Cheng J, et al. Dual atoms (Fe, F) Co-doping inducing electronic structure modulation of NiO hollow flower-spheres for enhanced oxygen evolution/sulfon oxidation reaction performance. *Small.* 2023;19(38):2302055.
136. Wang J, Ren Y, Wang P. (Fe, F) co-doped nickel oxyhydroxide for highly efficient oxygen evolution reaction. *J Mater Chem A.* 2023;11(9):4619-4626.
137. Gan Y, Ye Y, Dai X, et al. La and S Co-doping induced the synergism of multiphase nickel-iron nanosheets with rich oxygen vacancies to trigger large-current-density oxygen evolution and urea oxidation reactions. *Small.* 2023;19(46):e2303250.
138. Yin X, Dai X, Nie F, et al. Electronic modulation and proton transfer by iron and borate co-doping for synergistically triggering the oxygen evolution reaction on a hollow NiO bipyramidal prism. *Nanoscale.* 2021;13(33):14156-14165.
139. Li Y, Guo H, Zhang Y, Song R. Cooperative phosphorus and chromium doping induced electronic and morphological dual modulation in NiMoO₄ hydrate for energy-efficient urea-assisted hydrogen production. *Appl Catal B Environ.* 2024;341:123296.
140. Chen Z, Zheng R, Deng S, et al. Modular design of an efficient heterostructured FeS₂/TiO₂ oxygen evolution electrocatalyst via sulfidation of natural ilmenites. *J Mater Chem A.* 2021;9(44):25032-25041.
141. Jo S, Lee KB, Sohn JI. Direct electrosynthesis of selective transition-metal chalcogenides as functional catalysts with a tunable activity for efficient water electrolysis. *ACS Sustainable Chem Eng.* 2021;9(44):14911-14917.
142. Zhuo M, Chen Z, Liu X, Wei W, Shen Y, Ni B-J. A broad horizon for sustainable catalytic oxidation of microplastics. *Environ Pollut.* 2023;340:122835.
143. Chen Z, Wei W, Shen Y, Ni B-J. Defective nickel sulfide hierarchical structures for efficient electrochemical conversion of plastic waste to value-added chemicals and hydrogen fuel. *Green Chem.* 2023;25(15):5979-5988.
144. Ghising RB, Pan UN, Kandel MR, et al. Bimetallic-organic frameworks derived heterointerface arrangements of V, N co-doped Co/Fe-selenide nanosheets electrocatalyst for efficient overall water-splitting. *Mater Today Nano.* 2023;24:100390.
145. Chen J, Chen J, Cui H, Wang C. Electronic structure and crystalline phase dual modulation via anion-cation co-doping for boosting oxygen evolution with long-term stability under large current density. *ACS Appl Mater Interfaces.* 2019;11(38):34819-34826.
146. Chen Z, Zheng R, Bao T, et al. Dual-doped nickel sulfide for electro-upgrading polyethylene terephthalate into valuable chemicals and hydrogen fuel. *Nano-Micro Lett.* 2023;15(1):210.
147. Zheng X, Sun S, Liu Y, et al. Synergistic modulation of NiSe₂ by doping with chromium and nitrogen for high-efficiency overall water splitting. *Appl Surf Sci.* 2023;609:155406.
148. Hao J, Luo W, Yang W, Li L, Shi W. Origin of the enhanced oxygen evolution reaction activity and stability of a nitrogen and cerium co-doped CoS₂ electrocatalyst. *J Mater Chem A.* 2020;8(43):22694-22702.
149. Chen Y, Zhang X, Ma X, Wang Y. Modulation of bulk and surface electronic structures for oxygen evolution by Cr, P co-doped Co₃S₄. *Chem Commun.* 2023;59(50):7775-7778.
150. Jiang L, Gu M, Wang H, et al. Synergistically regulating the electronic structure of CoS by cation and anion dual-doping for efficient overall water splitting. *ChemSusChem.* 2023;16(18):e202300592.
151. Wang Y, Li S, Zhang D, Tan F, Li L, Hu G. Self-supported hierarchical P,Cu-codoped cobalt selenide nanoarrays for enhanced overall water splitting. *J Alloys Compd.* 2021;889:161696.
152. Zhang Y-Y, Zhang X, Wu Z-Y, et al. Fe/P dual doping boosts the activity and durability of CoS₂ polycrystalline nanowires for hydrogen evolution. *J Mater Chem A.* 2019;7(10):5195-5200.
153. Guo T, Lin Y, Chen X, et al. Metal-nonmetal atom co-doping engineered transition metal disulfide for highly efficient hydrogen evolution reaction. *Int J Hydrogen Energy.* 2023;48(8):2990-2997.
154. Ling M, Li N, Jiang B, et al. Rationally engineered Co and N co-doped WS₂ as bifunctional catalysts for pH-universal

- hydrogen evolution and oxidative dehydrogenation reactions. *Nano Res.* 2022;15(3):1993-2002.
155. Cao D, Ye K, Moses OA, et al. Engineering the in-plane structure of metallic phase molybdenum disulfide via Co and O dopants toward efficient alkaline hydrogen evolution. *ACS Nano.* 2019;13(10):11733-11740.
156. Zhan Y, Zhou X, Nie H, et al. Designing Pd/O co-doped MoS_x for boosting the hydrogen evolution reaction. *J Mater Chem A.* 2019;7(26):15599-15606.
157. Tian L, Pang X, Xu H, et al. Cation-anion dual doping modifying electronic structure of hollow CoP nanoboxes for enhanced water oxidation electrocatalysis. *Inorg Chem.* 2022;61(42):16944-16951.
158. Lin C, Wang D, Jin H, et al. Construction of an iron and oxygen co-doped nickel phosphide based on MOF derivatives for highly efficient and long-enduring water splitting. *J Mater Chem A.* 2020;8(8):4570-4578.
159. Li M-X, Ma Y, Xiao B, et al. S, Fe dual doped and precisely regulated CoP porous nanoneedle arrays for efficient hydrogen evolution at 3 A cm⁻². *Chem Eng J.* 2023;470:144081.
160. Jiang X, Yue X, Li Y, et al. Anion-cation-dual doped tremella-like nickel phosphides for electrocatalytic water oxidation. *Chem Eng J.* 2021;426:130718.
161. Zhao T, Wang S, Jia C, et al. Cooperative boron and vanadium doping of nickel phosphides for hydrogen evolution in alkaline and anion exchange membrane water/seawater electrolyzers. *Small.* 2023;19(27):2208076.
162. Zhang W, Sun Y, Liu Q, Guo J, Zhang X. Vanadium and nitrogen co-doped CoP nanoleaf array as pH-universal electrocatalyst for efficient hydrogen evolution. *J Alloys Compd.* 2019;791:1070-1078.
163. Zhang B, Wang L, Cao Z, et al. High-valence metals improve oxygen evolution reaction performance by modulating 3d metal oxidation cycle energetics. *Nat Catal.* 2020;3(12):985-992.
164. Yan Y, Liu C, Jian H, et al. Substitutionally dispersed high-oxidation CoO_x clusters in the lattice of rutile TiO₂ triggering efficient Co-Ti cooperative catalytic centers for oxygen evolution reactions. *Adv Funct Mater.* 2021;31(9):2009610.
165. Kim M, Min K, Ko D, Seong H, Eun Shim S, Baeck S-H. Regulating the electronic structure of Ni₂P by one-step Co, N dual-doping for boosting electrocatalytic performance toward oxygen evolution reaction and urea oxidation reaction. *J Colloid Interface Sci.* 2023;650:1851-1861.
166. Li J, Cui H, Du X, Zhang X. The controlled synthesis of nitrogen and iron co-doped Ni₃S₂@NiP₂ heterostructures for the oxygen evolution reaction and urea oxidation reaction. *Dalton Trans.* 2022;51(6):2444-2451.
167. Luo F, Shu X, Jiang X, Liu Y, Zhang J, Chen S. Accelerating the surface reconstruction of cobalt phosphide via dual-doping engineering for high-performance water electrolysis. *J Power Sources.* 2022;551:232181.
168. El-Refaei SM, Russo PA, Schultz T, Koch N, Pinna N. Dual doping of MoP with M(Mn, Fe) and S to achieve high hydrogen evolution reaction activity in both acidic and alkaline media. *ChemCatChem.* 2021;13(20):4392-4402.
169. Hoa VH, Tran DT, Nguyen DC, Kim DH, Kim NH, Lee JH. Molybdenum and phosphorous dual doping in cobalt monolayer interfacial assembled cobalt nanowires for efficient overall water splitting. *Adv Funct Mater.* 2020;30(34):2002533.
170. Xu W, Zhang J-P, Zhao S, et al. Cobalt and sulfur co-doping induce nickel electron localization to enhance alkaline hydrogen evolution activity. *Fuel.* 2023;352:129087.
171. Li P, Zheng D, Gao M, et al. Bimetallic MOF-templated fabrication of porous Zn, N Co-doped Mo₂C for an efficient hydrogen evolution reaction. *ACS Appl Energy Mater.* 2021;4(9):8875-8882.
172. Chen J, Jia J, Wei Z, et al. Ni and N co-doped MoCx as efficient electrocatalysts for hydrogen evolution reaction at all-pH values. *Int J Hydrogen Energy.* 2018;43(31):14301-14309.
173. Chen Z, Zheng R, Zou W, et al. Integrating high-efficiency oxygen evolution catalysts featuring accelerated surface reconstruction from waste printed circuit boards via a bordering recycling strategy. *Appl Catal B Environ.* 2021;298:120583.
174. Chen Z, Zou W, Zheng R, et al. Synergistic recycling and conversion of spent Li-ion battery leachate into highly efficient oxygen evolution catalysts. *Green Chem.* 2021;23(17):6538-6547.
175. Hong YR, Kim KM, Ryu JH, et al. Dual-phase engineering of nickel boride-hydroxide nanoparticles toward high-performance water oxidation electrocatalysts. *Adv Funct Mater.* 2020;30(38):2004330.
176. Chen Z, Zheng R, Wei W, et al. Recycling spent water treatment adsorbents for efficient electrocatalytic water oxidation reaction. *Resour Conserv Recycl.* 2022;178:106037.
177. Wang L, Li J, Zhao X, et al. Surface-activated amorphous iron borides (FexB) as efficient electrocatalysts for oxygen evolution reaction. *Adv Mater Interfac.* 2019;6(6):1801690.
178. Chen Z, Duan X, Wei W, Wang S, Zhang Z, Ni B-J. Boride-based electrocatalysts: emerging candidates for water splitting. *Nano Res.* 2020;13(2):293-314.
179. Liu Y, Vijayakumar P, Liu Q, Sakthivel T, Chen F, Dai Z. Shining light on anion-mixed nanocatalysts for efficient water electrolysis: fundamentals, progress, and perspectives. *Nano-Micro Lett.* 2022;14(1):43.
180. Anjum MAR, Bhatt MD, Lee MH, Lee JS. Sulfur-doped dicobalt phosphide outperforming precious metals as a bifunctional electrocatalyst for alkaline water electrolysis. *Chem Mater.* 2018;30(24):8861-8870.
181. He W, Liu H, Cheng J, et al. Modulating the electronic structure of nickel sulfide electrocatalysts by chlorine doping toward highly efficient alkaline hydrogen evolution. *ACS Appl Mater Interfaces.* 2022;14(5):6869-6875.
182. Zhou Y, Chu B, Sun Z, et al. Surface reconstruction and charge distribution enabling Ni/W₅N₄ Mott-Schottky heterojunction bifunctional electrocatalyst for efficient urea-assisted water electrolysis at a large current density. *Appl Catal B Environ.* 2023;323:122168.
183. Chen Z, Zheng R, Li S, et al. Dual-anion etching induced in situ interfacial engineering for high-efficiency oxygen evolution. *Chem Eng J.* 2021;431:134304.
184. Chen Z, Zheng R, Zou H, et al. Amorphous iron-doped nickel boride with facilitated structural reconstruction and dual active sites for efficient urea electrooxidation. *Chem Eng J.* 2023;465:142684.
185. Zhang X, Fang X, Zhu K, et al. Fe-doping induced electronic structure reconstruction in Ni-based metal-organic framework for improved energy-saving hydrogen production via urea degradation. *J Power Sources.* 2022;520:230882.

186. Yang D, Su Z, Chen Y, et al. Self-reconstruction of a MOF-derived chromium-doped nickel disulfide in electrocatalytic water oxidation. *Chem Eng J.* 2022;430:133046.
187. Wang J, Xuan H, Meng L, et al. Facile synthesis of N, S co-doped CoMoO₄ nanosheets as high-efficiency electrocatalysts for hydrogen evolution reaction. *Ionics.* 2022;28(10):4685-4695.
188. Fei M, Shi H, Zhao J, et al. Porous microspherical N and P-co-doped NiFe₂O₄/single-walled carbon nanotubes for efficient electrochemical oxygen evolution reaction. *Chem-CatChem.* 2018;10(22):5174-5181.
189. Ma X, Zhang S, He Y, et al. Boron and phosphorus co-doped NiVFe LDHs@NF as a highly efficient self-supporting electrocatalyst for the hydrogen evolution reaction. *J Electroanal Chem.* 2021;886:115107.
190. Zhao C, Li J, Yang M, et al. S/Se dual-doping promotes the formation of active Ni/Fe oxyhydroxide for oxygen evolution reaction of (sea)water splitting. *Int J Hydrogen Energy.* 2022;47(51):21753-21759.
191. Feng A, Ding S, Liu P, et al. N, P co-doping triggered phase transition of MoS₂ with enlarged interlayer spacing for efficient hydrogen evolution. *New J Chem.* 2022;46(32):15693-15700.
192. Liu J, Wang Z, Li J, Cao L, Lu Z, Zhu D. Structure engineering of MoS₂ via simultaneous oxygen and phosphorus incorporation for improved hydrogen evolution. *Small.* 2020;16(4):1905738.
193. Bai X, Wang Q, Xu G, et al. Phosphorus and fluorine co-doping induced enhancement of oxygen evolution reaction in bimetallic nitride nanorods arrays: ionic liquid-driven and mechanism clarification. *Chem Eur J.* 2017;23(66):16862-16870.
194. Doan TLL, Tran DT, Nguyen DC, Kim DH, Kim NH, Lee JH. Rational engineering Co_xO_y nanosheets via phosphorous and sulfur dual-coupling for enhancing water splitting and Zn-air battery. *Adv Funct Mater.* 2021;31(10):2007822.
195. Pan D-S, Guo Z-H, Li J-K, Huang S, Zhou L-L, Song J-L. Rational construction of a N, F Co-doped mesoporous cobalt phosphate with rich-oxygen vacancies for oxygen evolution reaction and supercapacitors. *Chem Eur J.* 2021;27(28):7731-7737.
196. Ang H, Tan HT, Luo ZM, et al. Hydrophilic nitrogen and sulfur co-doped molybdenum carbide nanosheets for electrochemical hydrogen evolution. *Small.* 2015;11(47):6278-6284.
197. Park K, Kwon J, Jo S, et al. Simultaneous electrical and defect engineering of nickel iron metal-organic-framework via co-doping of metalloid and non-metal elements for a highly efficient oxygen evolution reaction. *Chem Eng J.* 2022;439:135720.
198. Kim K, Kang T, Kim M, Kim J. Exploring the intrinsic active sites and multi oxygen evolution reaction step via unique hollow structures of nitrogen and sulfur co-doped amorphous cobalt and nickel oxides. *Chem Eng J.* 2021;426:130820.
199. Lee G, Kim J. Effective tri-metal and dual-doped catalyst for oxygen evolution reaction: amorphous Co-Mn-Ni-P-B-O nanoparticles. *Appl Surf Sci.* 2022;591:153171.
200. Wang X, He Y, Han X, et al. Engineering cobalt sulfide/oxide heterostructure with atomically mixed interfaces for synergistic electrocatalytic water splitting. *Nano Res.* 2022;15(2):1246-1253.
201. Kim G-Y, Lee J, Rho Y-J, et al. Rhenium oxide/sulfide binary phase flakes decorated on nanofiber support for enhanced activation of electrochemical conversion reactions. *Chem Eng J.* 2022;446:136951.
202. Du X, Shao Q, Zhang X. Cu-Co-M arrays on Ni foam as monolithic structured catalysts for water splitting: effects of co-doped S-P. *Dalton Trans.* 2019;48(4):1322-1331.
203. Sun K, Zeng L, Liu S, et al. Design of basal plane active MoS₂ through one-step nitrogen and phosphorus co-doping as an efficient pH-universal electrocatalyst for hydrogen evolution. *Nano Energy.* 2019;58:862-869.
204. Maiti A, Srivastava SK. Sulphur Sulfur edge and vacancy assisted nitrogen-phosphorus co-doped exfoliated tungsten disulfide: a superior electrocatalyst for hydrogen evolution reaction. *J Mater Chem A.* 2018;6(40):19712-19726.
205. Anjum MAR, Lee JS. Sulfur and nitrogen dual-doped molybdenum phosphide nanocrystallites as an active and stable hydrogen evolution reaction electrocatalyst in acidic and alkaline media. *ACS Catal.* 2017;7(4):3030-3038.
206. Kim SH, Yoo SH, Shin S, et al. Controlled doping of electrocatalysts through engineering impurities. *Adv Mater.* 2022;34(28):2203030.

AUTHOR BIOGRAPHIES



Zhijie Chen received his Ph.D. degree in Environmental Engineering from the University of Technology Sydney, Australia in 2022. He now works as a postdoctoral researcher at the University of New South Wales, Sydney. His research mainly work focuses on the development of cost-effective functional materials for advanced energy and environmental applications (e.g., (waste) water electrolysis, plastic waste upcycling).



Bing-Jie Ni received his Ph.D. degree in environmental engineering in June 2009. He currently is a full professor at the University of New South Wales, Sydney. He is a Fellow of the Royal Society of Chemistry and a Clarivate Global Highly Cited Researcher. His work focuses on the integration of different disciplines to develop innovative and sustainable technological solutions to achieve environmental and energy sustainability.

How to cite this article: Chen Z, Han N, Wei W, Chu D, Ni B-J. Dual doping: an emerging strategy to construct efficient metal catalysts for water electrolysis. *EcoEnergy.* 2024;2(1):114-140. <https://doi.org/10.1002/ece2.29>